AD_____

GRANT NUMBER: DAMD17-94-J-4444

TITLE: Spatial Distribution of the EGF Receptor in Regulation of Breast Epithelial Cell Growth and Organization

PRINCIPAL INVESTIGATOR: H. Steven Wiley, Ph.D.

CONTRACTING ORGANIZATION: University of Utah
Salt Lake City, UT 84102

REPORT DATE: September 1996

TYPE OF REPORT: Annual

PREPARED FOR: Commander
U.S. Army Medical Research and Materiel Command
Fort Detrick, Frederick, MD 21702-5012

REPORT DOCUMENTATION PAGE

Form Approved
OMB No. 0704-0188

1. AGENCY USE ONLY *(Leave blank)*	2. REPORT DATE	3. REPORT TYPE AND DATES COVERED
	March 1997	Annual (1 Sep 95 - 31 Aug 96)

4. TITLE AND SUBTITLE
Spatial Distribution of the EGF Receptor in Regulation of Breast Epithelial Cell Growth and Organization

5. FUNDING NUMBERS
DAMD17-94-J-4444

6. AUTHOR(S)
H. Steven Wiley, Ph.D.

7. PERFORMING ORGANIZATION NAME(S) AND ADDRESS(ES)
University of Utah
Salt Lake City, UT 84102

8. PERFORMING ORGANIZATION REPORT NUMBER

9. SPONSORING/MONITORING AGENCY NAME(S) AND ADDRESS(ES)
Commander
U.S. Army Medical Research and Materiel Command
Fort Detrick, MD 21702-5012

10. SPONSORING/MONITORING AGENCY REPORT NUMBER

11. SUPPLEMENTARY NOTES

12a. DISTRIBUTION / AVAILABILITY STATEMENT
Approved for public release; distribution unlimited

12b. DISTRIBUTION CODE

13. ABSTRACT *(Maximum 200)*

Growth factors provide important information to cells and the spatial distribution of growth factor receptors is important in this process. We disrupted the normal distribution of receptor-ligand interactions by introducing into nontransformed human mammary epithelial cells an oncogenic form of the EGF receptor that is constitutively active and undergoes abnormal trafficking. We also introduced a mutant form of EGF which can bind to the receptor inside of the cell (intracrine signaling). We found that the oncogenic EGF receptor actually inhibited cell growth and division, whereas the mutant EGF stimulated growth. Both mutant receptors and ligands disrupted normal organization and response of the cells to the extracellular environment. In this way the cells resembled breast cancer cells. Our results indicate that oncogenic growth factor receptors do not necessarily stimulate mitogenesis, but may instead work by inhibiting normal environmental sensing. This in turn may lead to uncontrolled cell proliferation.

14. SUBJECT TERMS
Breast Cancer

15. NUMBER OF PAGES
64

16. PRICE CODE

17. SECURITY CLASSIFICATION OF REPORT	18. SECURITY CLASSIFICATION OF THIS PAGE	19. SECURITY CLASSIFICATION OF ABSTRACT	20. LIMITATION OF ABSTRACT
Unclassified	Unclassified	Unclassified	Unlimited

FOREWORD

Opinions, interpretations, conclusions and recommendations are those of the author and are not necessarily endorsed by the US Army.

__✓__ Where copyrighted material is quoted, permission has been obtained to use such material.

__✓__ Where material from documents designated for limited distribution is quoted, permission has been obtained to use the material.

__✓__ Citations of commercial organizations and trade names in this report do not constitute an official Department of Army endorsement or approval of the products or services of these organizations.

____ In conducting research using animals, the investigator(s) adhered to the "Guide for the Care and Use of Laboratory Animals," prepared by the Committee on Care and Use of Laboratory Animals of the Institute of Laboratory Resources, National Research Council (NIH Publication No. 86-23, Revised 1985).

____ For the protection of human subjects, the investigator(s) adhered to policies of applicable Federal Law 45 CFR 46.

__✓__ In conducting research utilizing recombinant DNA technology, the investigator(s) adhered to current guidelines promulgated by the National Institutes of Health.

__✓__ In the conduct of research utilizing recombinant DNA, the investigator(s) adhered to the NIH Guidelines for Research Involving Recombinant DNA Molecules.

__✓__ In the conduct of research involving hazardous organisms, the investigator(s) adhered to the CDC-NIH Guide for Biosafety in Microbiological and Biomedical Laboratories.

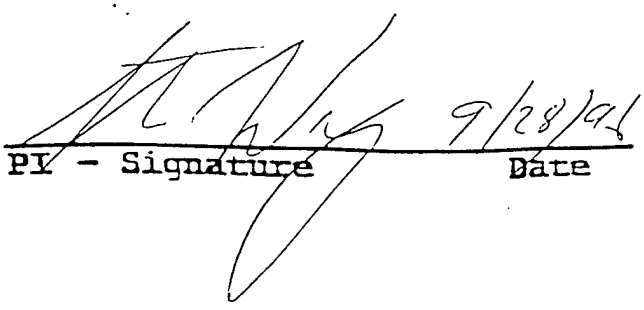

PI - Signature 9/28/94 Date

TABLE OF CONTENTS

INTRODUCTION.....

An important goal of current breast cancer research is to develop an in vitro system that can define the mechanisms involved in the progression of human mammary epithelial cells (HMEC) towards a transformed phenotype. In this project, we have focused on an aspect of HMEC behavior that is likely to be involved in this progression, namely, the correct spatial sorting of growth factors and their receptors to discrete cellular locations. We chose this research focus for two important reasons: 1) recent evidence indicates that defects in receptor/ligand trafficking is a hallmark of proliferative disorders in epithelial cells (1,2), and 2) since receptor trafficking is primarily a negative regulatory process defects in this pathway are likely to amplify receptor signaling (3,4). Because correct receptor trafficking depends on the function of many intracellular regulatory systems, it provides a sensitive readout of their status. The EGF receptor system is used as the primary experimental model because it plays a central role in the growth, motility and proliferation of normal HMEC as well as many breast cancers (5-8). Therefore any significant alterations in growth factor regulation in HMEC is likely to perturb the EGF receptor system.

The functions of growth factors extend far beyond simple growth regulation. They are involved in cell differentiation, chemotaxis, morphogenesis, wound healing and gastric acid secretion (9). Originally, growth factors were thought to be products secreted by cells, but in fact, many are produced as membrane-associated precursors. For example, EGF is initially produced as a 170 kDa membrane protein (10) and transforming growth factor alpha (TGF-α) is produced as a 20-22 kDa MW precursor (11). In the case of TGF-α, release from the cell surface occurs through regulated proteolysis (12). The multiple levels at which availability of growth factors can be regulated provide many opportunities for fine control of tissue functions.

Three main routes of growth factor signaling are currently recognized: autocrine, paracrine and juxtacrine (13). In autocrine signaling, cells make both the growth factor and the complementary receptors. In general, the factors must be transported to the cell surface to be functional. In paracrine signaling, different cells make the ligand and receptors. The factor must be transported from the site of production to the site of binding, usually by diffusion. Finally, juxtacrine signaling occurs when receptors on one cell bind directly to the membrane-associated ligand on another cell. All of these types of signaling can be regulated by controlled synthesis, rate of ligand release, and by competition for ligand capture either between different cells or by extracellular matrix proteins (13). Growth factor signaling is also regulated by the physical separation of the ligand and receptor at the cell surface or within the endocytic pathway. This spatial regulation is mediated by sorting components which bind to receptor cytoplasmic domains (14). Growth factors may also be synthesized initially as transmembrane proteins, presumably allowing cells to physically segregate them from receptors.

Epithelial cells display a high degree of spatial organization as evidenced by their polarized phenotype. Kidney, breast and intestinal epithelial cells all show similar features; all are associated through tight junctions and have distinct basolateral and apical surfaces (15). In-vivo, breast epithelium is organized into ducts, ductules and alveoli consisting of a basement membrane, a discontinuous layer of myoepithelial cells, a layer of basal epithelial cells and a layer of luminal cells (16). Both basal and luminal cells display a polarized distribution of integrins and EGF-R (17-19). Integrins mediate interactions with the basement

membrane and appear essential for controlling specific gene expression and maintaining polarization and differentiated functions (20,21). EGF-R are important in regulating epithelial cell growth, and in the breast, are expressed at high levels in myoepithelial cells, basal cells and at the basolateral surface of luminal epithelial cells (19). The functional significance of the basolateral distribution of these receptors is not understood, but could be involved in maintaining the correct organization of epithelial cells within tissues.

Three ligands are thought to be produced in mature breast alveoli which can bind to the EGF-R: EGF, TGF-α and amphiregulin (5,22,23). The best studied of these, TGF-α, is produced by epithelial cells and at least in the mouse, is localized at their basolateral surface (24). Because the basolateral surface contains the EGF-R, the space between this surface and the basement membrane comprises the "microenvironment" in which signaling through the EGF-R occurs. Although EGF is found at high concentrations in the ductal lumen of both mouse and human, little TGF-α is found in breast milk or nipple aspirates of humans (approximately 0.8 ng/ml and 5 ng/ml respectively), indicating a polarized secretion of EGF to the apical surface and TGF-α to the basolateral surface of luminal cells (25). Nothing is known regarding the distribution of amphiregulin in HMEC, but in intestinal cells it displays a luminal distribution (26). Significantly, an extremely high concentration of EGF is found in breast fluids of non-lactating (>200ng/ml) or lactating (100-140 ng/ml) women (25). These concentrations are 2 orders of magnitude higher than the K_d of the EGF-R in HMEC. Therefore, the polarized organization of HMEC segregates their EGF-R from a large reservoir of active hormone.

Ligand activation of EGF-R leads to heterodimer formation between EGF-R and erbB-2, which is thought to result in activation of erbB-2 by transphosphorylation (39-40). Transactivation of erbB-2 also occurs upon the addition of heregulin, a ligand for erbB-3 and erbB-4 (41-44). As observed for EGF, heregulin induces the formation of heterodimers between erbB-3 or erbB-4 with erbB-2, resulting in erbB-2 becoming tyrosine phosphorylated (42, 43 45, 46, 48). There is also evidence to suggest that EGF-R interacts with erbB-3 and erbB-4 (49). Thus, activation of any member of the EGF-R family results in signaling through multiple receptor types. Understanding how these receptors interact with each other is therefore essential to knowing how they work.

The pattern of tyrosine phosphorylation of EGF-R and erbB-2 is important in signal transduction. Specific phosphorylated tyrosines residues serve as docking sites for proteins containing SH2 domains, such as the PI3 kinase p85 subunit and GRB2 (45). The assembly of signaling complexes dictates the subsequent pattern of signal transduction. Intracellular trafficking of the activated EGF-R also regulates receptor activity by controlling the availability of substrates and signaling partners (50). Although ligand binding induces rapid internalization and subsequent lysosomal targeting of EGF-R, it is uncertain whether erbB-2 trafficking is influenced by the EGF-R. It has been suggested that all members of the erbB family are "internalization defective" except for the EGF-R (51), but those studies were done by direct activation of erbB family members or by using chimeric receptors. It has been reported that EGF treatment can stimulate the degradation of erbB-2 in some epithelial cells, but the mechanism of this transmodulation is unclear (52). If EGF-R activation does alter the trafficking of erbB-2, this could be an important mechanism for regulating both the activity and distribution of these signaling molecules in cells. However, the degree of spatial overlap between the members of the EGFR family in mammary epithelial cells is unknown.

The correct distribution of the EGFR within a cell is also very important in regulating signal transduction. Receptors that are mutated to remove sequences that specify receptor internalization can be transforming (4). This is presumably due to an inability to down regulate and thus attenuate signaling from the mutant receptor. However, these mutant receptors may also have access to inappropriate substrates which may contribute to the transformed phenotype.

A great many studies have investigated the relationship between EGF-R and breast cancer (8,19, 27,28). In general, overexpression of the EGF-R in breast tumors indicates poor prognosis, but other growth factor receptors, such as HER2/*neu*, also appear to be linked to breast cancer (8). The incidence of overexpression of the EGF-R is more common than overexpression of HER2/*neu* (45% versus 20% respectively; (8)). Significantly, less than 20% of the tumors that display overexpression of the EGF-R also show amplification of the EGF-R gene, whereas all incidents of HER2/*neu* overexpression appear to be due to gene amplification (29). This indicates that the EGF-R is subject to multiple levels of control that can be independently altered during transformation. Tight control on the EGF-R system is probably necessary because it appears to be the major regulator of HMEC proliferation in vivo. EGF-containing pellets can stimulate normal ductal growth in regressed mammary glands of ovariectomized mice (24). Estrogens appear to regulate the proliferation of HMEC in vivo and in vitro in part through an EGF-R autocrine loop (30,31). Blocking EGF-R occupancy in vitro using a monoclonal antibody causes HMEC to reversibly enter G_0(6). EGF is essential for the motility and assembly of HMEC into organized alveolar structures in vitro. EGF also has a dual effect of promoting growth and chemotaxis/motility of keratinocytes (32) and intestinal epithelial cells (33), suggesting that it has a general role in both establishing and maintaining the structure of epithelial tissues. Recently, rearrangements of the EGF-R have been found in 78% of breast carcinomas (34), again implicating the activity of this receptor in transformation of breast epithelial cells.

Because of the importance of the EGF-R in HMEC regulation, it appears likely that genetic alterations that give HMEC a growth advantage will operate either directly or indirectly through this receptor system. Despite the numerous studies on EGF-R and breast cancer, this idea has not been critically tested. Studies that document the presence or absence of EGF-R (or their overexpression) are not particularly informative in this regard. For example, the MCF-7 breast cancer cell line displays very low levels of EGF-R expression compared to normal HMEC, but estrogen can induce proliferation in these cells in part through an EGF-R/TGF-α autocrine pathway (35). In rapidly proliferating HMEC, there is a positive relationship between TGF-α levels and proliferation, apparently due to a positive feedback loop operating through the EGF-R (5). Amphiregulin and EGF-R levels are also high in proliferating HMEC, but not in intact organoid structures (5,23). Control of receptor number could regulate other aspects of HMEC function, such as directional sensing of ligands. In addition, genetic lesions that operate downstream of the EGF-R itself would not necessarily affect receptor expression. The present uncertainty regarding the role, if any, of the EGF-R in breast cancer reflects our general lack of understanding of its role in normal epithelial cell function, an issue directly addressed by our studies.

Over the last year, we have make progress in our efforts to understand the role of the EGFR in both tissue organization and cancer. We have found that oncogenic forms of the EGFR do not act as normal, ligand-activated receptors, but instead have unique activities. We have found that autocrine signaling is crucial in normal organization of HMEC. In particular, the regulated

release and selective interruption of autocrine loops provide cells with important spatial clues regarding their environment. Finally, we have extended our studies to other members of the EGFR family important in breast cancer, such as erbB-2. We found that spatial regulation of the EGFR may directly affect signaling through erbB-2. Taken together, our studies have significantly enhanced our understanding of the role of the EGFR in normal and transformed HMEC.

BODY

We have revised our original statement of work. The original tasks were:

> Task 1: Define the Changes That Occur in the Spatial Organization of Both the EGF-R and its Ligands During Formation of Organized Alveolar Structures in Vitro (Months 1-24)
>
> Task 2: Determine Whether a Loss in the Correct Spatial Organization of the EGF Receptor is Associated with a Loss of Specific Tumor Suppressor Genes (Months 12-36)
>
> Task 3: Express genetically altered EGF receptors in mammary epithelial cells (Months 12-36)
>
> Task 4: Demonstrate That Mis-sorting or Inappropriate Expression of the EGF Receptor or its Ligands Provides a Growth Advantage to Normally Organized Epithelial Cells (Months 24-48)

The new tasks are:

> Task 1: Determine the normal pattern of compartmentation and regulation of EGF and its ligands in nontransformed mammary epithelial cells. Define the extent to which this is similar to the pattern described for other cell types and define conditions under which these cells form organized alveolar structures. (Months 1-24)
>
> Task2: Determine whether oncogenic forms of the EGF receptor found in breast cancer display the same pattern of spatial regulation and biological activity as activated, wild type EGF receptors (Months 12-36)
>
> Task3: Express genetically altered EGF receptors and ligands in mammary epithelial cells (Months 12-36)
>
> Task 4: Demonstrate that mis-sorting or inappropriate expression of the EGFR or its ligands provides a growth advantage to HMEC or inhibit normal organization (Months 24-48)
>
> Task 5: Determine how the pattern of spatial regulation of the EGFR affects its ability to transactivate and transmodulate erbB-2 (Months 12-36)

These minor changes in the statement of work were necessatated by several observations made

during the course of this investigation. With respect to Task 1, we found that organization of HMEC into alveolar structures was not sufficiently reproducible to allow us to definitely establish how organization of the EGFR and its ligands changed during this process. The lack of reproducibility was primarily due to the nature of Matrigel, which is used as the matrix to induce cell organization. Matrigel is isolated from EHS tumors grown in mice and is a complex mixture of matrix components. The composition of this material changes from batch to batch. Organization of HMEC on this material is highly dependent on cell density because of the competing processes of cell-cell contact and cell-matrix contact and degradation as a function of time. Depending on the composition of a given batch of Matrigel, a different cell density was required to achieve given level of organization. This type of variation made it impossible to pool results from different experiments or to accurately define changes occurring within cells at any given position within the structure. The work we did on this aim was not wasted, however, because we found that alterations in oncogene expression in HMEC had significant effects on their ability to organize. We used this observation to expand the scope of task 4.

As redefined, Task 1 involves the development and characterization of the central model system of this proposal. In the previous progress report, we demonstrated the feasibility of the molecular and biochemical techniques needed for this project. In the current report, we describe the assays needed to investigate the growth and organization of the cells (see below).

Task 2 was altered because of significant new findings by other investigators on oncogenes related to the EGFR that may be involved in breast cancer. At the time this proposal was submitted, there was little information available on which oncogenes involved in breast cancer may interact with the EGFR pathway. We therefore proposed to examine the interaction of several "best guess" candidates. Since that time, two significant findings have been made. The first finding was that a rearranged, oncogenic form of the EGFR itself has been found in over 70% of breast cancer (34). Because the spatial regulation of this receptor has been reported to differ from that observed for the wild-type EGFR (53), it seemed appropriate to investigate this receptor in the context of this proposal. One publication has already resulted from this study (53) and another one is current in preparation (see below). The second finding was that members of the EGFR family interact extensively, forming homo- and heterodimers. Of particular interest was the finding that erbB-2 (also known as HER2 and neu) does not appear to be activated by binding a ligand, but by forming heterodimers with other members of the EGFR family. This is highly significant with regard to breast cancer, because overexpression of erbB-2 indicates poor prognosis. In keeping with the theme of the current proposal, we have focused on understanding the role of spatial regulation of the EGFR on the transactivation and transmodulation of erbB-2. We have therefore added a Task 5 to the SOW. This new line of investigation has been extremely productive. It has already resulted in one publication in press (R. Worthylake and H. S. Wiley. Structural aspects of the epidermal growth factor receptor required for transmodulation of erbB-2/neu. J. Biol. Chem. 1997 Mar 28; 272 (13): 8594). Progress in this line of investigation continues to be productive.

The other two tasks remain the same and we continue to make excellent progress. The reviewers of our progress report have criticized us for our inability to achieve polarized monolayers of mammary epithelial cells in transwell cultures. Such an achievement was never proposed in the original SOW and has proven elusive to us and all investigators in the field. It may indeed be a physical impossibility to achieve electrically tight junctions of HMEC growing in transwell cultures. However, we consider this a methodological problem. "Spatial regulation" is a broad term that refers to the distribution of EGFR between different cellular

compartments as well as apical and basolateral distributions. Because recent data indicates that the correct distribution of the EGFR between different cellular compartments is crucial to regulating cell growth and signal transduction, we feel that investigating these processes in the context of breast cancer is justified.

TASK 1 In the first progress report, we described molecular and biochemical aspects of EGFR regulation in nontransformed HMEC. As requested by the reviewers of our second progress report, we are including information describing the organization of HMEC on matrigel.

Materials and Methods - Reconstituted extracellular matrix derived from Englebreth-Holmes-Swarm fibrosarcoma (Matrigel) was purchased from Collaborative Research (Cambridge, MA). Monoclonal antibody 225 against the EGF-R (54) was purified from hybridomas obtained from the American Type Culture Collection. Human EGF was purchased from PreProTech, Inc. All other chemicals were purchased from Sigma.

Normal human mammary epithelial cells (HMEC) strain 184 and the immortalized cell line 184A1 were obtained from Dr. Martha Stampfer. The cells were cultured in serum free medium MCDB 170 prepared as described (6).

Matrigel was equilibrated by dialysis against MCDB 170 basal medium at 4°C. Cells are plated at a density of 200, 000 cells/well of a 12 well plate, with each well coated with 0.7 ml of Matrigel. After plating, the cells are examined daily and photographed. Wells contained medium without EGF, with 12.5 ng/ml EGF, or with 10 μg/ml 225 anti-EGFR antibody. Histologic sections were prepared by digesting cultures with collagenase - dispase. Intact colonies were then fixed in Bouin's fixative, embedded in paraffin, sectioned, and stained with hematoxylin and eosin.

Time-lapse photography as performed using a Sony video camera attached to a Wild dissection microscope through a video camera adaptor. A Panasonic commercial VHS time-lapse tape deck was used to acquire images. The recorder was triggered through a TTL relay (Alpha Electronics) attached to a Macintosh computer through its serial port. A BASIC program was written to acquire individual frames at the appropriate time intervals.

Results and Discussion - Human mammary epithelial cells (HMEC) strain 184 form a contact inhibited simple monolayer when grown under standard conditions on plastic tissue culture surfaces (Figure 1A). When plated on extracellular matrix derived from Englebreth-Holmes-Swarth fibrosarcoma (Matrigel), however, 184 cells rapidly assemble into epithelial cords to form complex three dimensional structures. Colonies mature over 6 to 10 days to form a complex tubular - branched network with multiple end buds that superficially resemble alveolar complexes *in vivo* (Figure 1B). Sections of mature structures revealed histologic features of adenosquamous differentiation (Figure 2). More pronounced squamous differentiation was seen after prolonged incubation, consistent with terminal squamous differentiation of senescent epithelial cells.

Video time lapse photography revealed a dynamic process in which structures mature through several distinct phases (Figs 3 & 4). Single cells rapidly migrate across the matrix surface during the first 24 hours after plating on Matrigel. Cell - cell contact induced cell spreading and proliferation in small aggregates, and cell movement across the matrix surface ceased as small aggregates formed (Fig 3). Large, macroscopic aggregates appeared during the next several days in a process that apparently involves remodeling of the extracellular matrix. Time lapse photography revealed *en bloc* movement of cellular aggregates and contraction of

the extracellular matrix around stable structures (Fig. 4). All cellular movement within the matrix stopped after several days as the relatively simple tubular - branched structures stabilized. The epithelial structures achieved their final form as large buds (approximately 40 to 50μm) grew over 5 to 7 days without further evidence of aggregate movement.

Because EGFR occupancy is important for the growth of HMEC, we were interested in determining its role in HMEC organization on Matrigel. Because 184 cells produce transforming growth factor-α and other ligands for the EGFR, we inhibited autocrine receptor activation by removing EGF from the culture medium and blocking autocrine ligand binding with a blocking antibody (225) against the EGFR. Interrupting the EGFR autocrine loop inhibited all phases of HMEC organization on Matrigel (Figure 5). HMEC remained as small groups of cells when plated on Matrigel in the absence of EGF and the presence of 225 antibody. There was no evidence of epithelial organization during prolonged incubation of these cultures.

We examined the effect of both EGF and antagonistic 225 antibody on the early phases of organization by using thin layers of Matrigel. Cells were plated at a low density and then examined 18 h later. As shown in Fig. 6 individual cells adhered to the layer of Matrigel in the absence of EGF, but did not spread. When two or more cells were in contact during plating, they spread, underwent rapid migration and recruited cells into a growing cell mass (Fig. 6, left panel). In the presence of exogenous EGF, all cells spread and migrated when plated on Matrigel (middle panel). In the presence of 225 mAb, no cells were able to spread or migrate (right panel). We conclude that EGF promotes spreading and cell migration on Matrigel. Interestingly, in the absence of exogenous EGF, only cells contacting a neighboring cell are able to respond to autocrine growth factors.

From these studies, we conclude that normal organization of HMEC on a basement membrane requires activation of the EGFR. The process of organization is complex and involves cell movement, proliferation and differentiation. Because blocking the EGFR stops many different cell processes, it was not possible to determine the level at which EGF exerted its effect. The results of this study encouraged us to take a more subtle approach in disrupting EGFR activation. In particular, we initiated a series of studies to determine whether the spatial pattern of EGFR ligand production was important in specifying the spatial pattern of cell organization (see task 3 below).

Task2: Determine whether oncogenic forms of the EGF receptor found in breast cancer display the same pattern of spatial regulation and biological activity as activated, wild type EGF receptors. This receptor (Δ2-7 EGFR), which lacks a portion of the extracellular binding domain encompassing exons 2-7, has been found in late stage glioblastoma multiforme disease where it occurs in up to 50% of grade IV tumors. It has also been found in 15% of non-small cell lung carcinomas and in 50-70% of breast and ovarian cancers (34). It thus appears to be a gene that is very relevant to breast cancer. The few studies published on the role of this receptor have examined its function in cells that do not require EGF for their growth as do HMEC.

We have recently shown that the enhanced tumorigenic activity of the Δ2-7 EGFR is due in part to an inability to be internalized and thus down regulated (53). An assumption of this study was that the Δ2-7 EGFR would act as a ligand-occupied EGFR and thus would be negatively regulated by the same processes. If this is the case, then the Δ2-7 EGFR would relax the normal requirement for activated EGFR in HMEC. This would be predicted to provide a

significant growth advantage to any putative "premalignant" cell carrying such a mutation. Alternately, the Δ2-7 EGFR could activate unique signaling pathways relative to the wild type receptor, perhaps offering an explanation as to why normal attenuation mechanisms are not activated. In either case, understanding the mechanistic basis of the transforming activity of the Δ2-7 EGFR is necessary to devise effective therapies for cells expressing this oncogene.

We therefore expressed the Δ2-7 EGFR in nontransformed HMEC. If they indeed behave the same as ligand-activated EGFR, then we would expect it to substitute for EGF. If they display unique activity, then we expect to observe altered behavior of the cells.

Materials and Methods

HMEC 184A1L5 cells grown in medium DFCI-1 were transduced with retrovirus containing the Δ2-7 EGF-R and G418 resistance (a kind gift of H.-J. Su Huang of the Ludwig Cancer Institute). They were selected in medium containing 100 μg/ml G418 and examined by flow cytometry for the presence of Δ2-7 at the cell surface which was detected using the Δ2-7 specific monoclonal antibody D806 followed by FITC-labeled secondary antibody. The levels of fluorescence of the transduced cells were compared to parental cells and indicated that a small population of cells did express the oncogenic receptor. Subsequent to FACS analysis the cells were diluted to clonal densities and grown in medium containing G418 until enough cells were generated to permit analysis by Western blot.

Western blot samples were obtained by scraping cells into a small volume (1 ml) of DMEM medium containing 25 mM Hepes buffer and the protease inhibitors pepstatin, chymostatin, aprotinin, leupeptin and iodoacetic acid followed by centrifugation to pellet the cells. Pelleted cells were extracted in a small volume of 1% Triton X-100, 50 mM Tris pH 7.2, 150 mM NaCl and the protease inhibitors mentioned above (100ug/ml). The clarified cell extracts were boiled in 2% SDS and placed onto 5-15% gradient gels. After electrophoresis the samples were transferred to nitrocellulose and probed with the N13 polyclonal antibody that recognizes both the mutant and wild-type receptor. Anti-phosphotyrosine blots were done using the RC20 genetically engineered anti-PY antibodies from Transduction Laboratories. Anti-SHC antibodies (rabbit) and anti-rabbit IgG-HRP were also from Transduction laboratories. Blots were developed using the ECL reagents from Pierce. A polyclonal anti-phosphotyrosine antibody generated by Chemicon using laboratory-synthesized antigen was also used.

Growth curves were generated by counting cell samples every 24 hour using a Coulter counter. Prior to starting the measurements, cells were maintained for 48 h in DFCI-1 medium lacking EGF. At time zero a cell sample was taken and either 10 μg/ml monoclonal antibody 225 or 12.5 ng/ml EGF was added to duplicate plates of cells. Cell counts were taken over a 5 day period.

Clonal growth assays were done by diluting confluent cultures of cells 1:800 into 60 mm dishes and allowing them to grow for three weeks in the presence of control medium (DFCI-1), or with either 10 μg/ml monoclonal antibody 225 or 12.5 ng/ml EGF. The cells were then stained with crystal violet.

Wound healing assays were performed by scraping cells from 60 mm plates at time zero and then measuring the distance recolonized every 24 h. Measurements were made using a Wild dissecting microscope with an ocular micrometer mounted in the eyepiece. Cells were cultured overnight in the absence of hormone prior to day zero and then placed into fresh medium after scraping.

Immunoprecipitation of WT and Δ2-7 EGFR was accomplished using Sepharose beads to which were coupled the appropriate antibody. Antibodies were coupled to Protein A Sepharose beads using a rabbit anti-mouse antibody as an intermediate. The antibodies were cross-linked to the beads using dimethyl pimelimidate. After washing the beads they were added directly to cell extracts (made as described above) and the mixture rocked for 1.5 h at 4°C. The beads were washed 5X with a solution containing 300 mM NaCl, 0.1% SDS, 0.05% NP40 and 10 mM Tris pH 8.3 and then boiled in SDS-PAGE sample buffer. SHC was immunoprecipitated from cell extracts using a polyclonal anti-SHC antibody (Transduction Laboratories). Cell extracts were prepared from 100 mm plates of washed cells by scraping the cells into a 1.5 ml volume of PBS containing 25 mM Hepes buffer and 1 mg/ml BSA as well as 10 μg/ml of the protease inhibitors pepstatin, chymostatin, aprotinin and leupeptin and 1 mM sodium orthovanadate and 10 mM NaF. After centrifugation and resuspension in PBS containing protease and phosphatase inhibitors, cells were recentrifuged and then extracted with 250ul Triton extract buffer (1% Triton X-100, 150 mM NaCl, 10% glycerol, 10 mM Na pyrophosphate, 1 mM EGTA, 4 mM iodoacetate, 1 mM orthovanadate, 10 mM NaF, 100 μg/ml pepstatin, chymostatin, aprotinin and leupeptin 50 mM HEPES, pH 7.0,). After 10 min on ice the extracts were centrifuged at 18,500xg for 10 min at 4°C and the supernatant removed. Protein concentration was determined using the BCA reagent kit (Pierce) and all samples were adjusted to equal protein levels. Extracts were incubated with preimmune rabbit IgG coupled to Protein A Sepharose for 30 min, centrifuged and 2.5 μg of anti-SHC antibody was added. After 60 min on ice, Protein A Sepharose was added and the samples rocked for 60 min in a cold room. After centrifugation, the Protein A beads were washed twice in 1% Triton X-100 buffer and then boiled in SDS sample buffer. Samples were electrophoresed on 5-15% gradient gels and transferred to nitrocellulose. The resulting Western blots were probed with RC20 anti-phosphotyrosine antibody (Transduction Laboratories) as described above.

Results and Discussion

Eighteen G418 resistant clones were generated by transduction with retrovirus. Initially, FACS analysis revealed that only a small proportion of cells transduced with virus were positive for the mutant receptor. This result was probably not accurate because the antibody directed against the mutant receptor also mildly cross-reacted with the endogenous wild type receptor. Since these cells express a large number of wild type EGF-R it resulted in a relatively large signal and obscured the positive signal from the Δ2-7 EGFR. Since we repeated this result several times, we went ahead with the cloning of the G418 resistant cells despite a seemingly disappointing transduction efficiency.

The Western blot quantification of receptor expression in Δ2-7 EGFR clones (Fig. 7) revealed that there were 9 positive clones expressing a wide range of mutant receptor mass (see Table 1). Expression of Δ2-7 EGF-R ranged from 15% of endogenous receptor levels up to clones in which there was 3-fold more mutant than wild type receptor. For future studies we chose to examine 3 or 4 different clones - #2 in which there are about equal levels of mutant and wild type receptor, #5 in which one quarter of the receptors are mutant, #16 in which one fifth are mutant and #11 in which three quarters of the receptors are mutant.

Percent total EGFR as D2-7 variant by clone															
Clone No.	1	2	3	4	5	6	7	8	9	10	11	12	16	17	19
% D2-7	50	50	15	21	25	0	0	0	0	25	76	0	19	0	43

We have compared the responses of parental HMEC184A1L5 cells with those of the Δ2-7 EGFR transduced cells described above. We have also included an additional control cell, one that expresses a secreted form of EGF (see Task 4 below). Ligand production in these cells is unregulated and results in chronic occupancy of the EGF-R. Cells were plated at clonal density and grown for 3 weeks. As shown in Fig. 8, parental HMEC184A1L5 (WT) cells grew well in the presence or absence of EGF (due to their active autocrine loop), but were blocked from growing by the antagonistic 225 anti-EGFR mAb. Cells making a non-membrane bound form of EGF (sEGF) grew well in the absence of EGF and well in the presence of 225 mAb, indicating a "short-circuited" autocrine loop (see task 4 below). Surprisingly, cells expressing the Δ2-7 EGFR grew quite poorly in the absence of EGF and did not grow at all in the presence of 225 mAb. The addition of EGF partially restored their growth. This result indicates that the Δ2-7 EGFR does not substitute for a ligand-occupied WT EGFR.

We also examined the growth rate of these cells. As shown in Fig. 9, cells expressing high numbers of Δ2-7 EGF-R grew at a much slower rate than the parental cells. When the EGF-R was blocked by 225 antibody, both cell clones expressing the mutant receptor were more sensitive to the effects of the antibody and grew at appreciably slower rates. Taken together these results refute the idea that the Δ2-7 EGF-R can eliminate the requirement for EGF in these cells. If anything, the presence of this receptor renders the cells less sensitive to the ligand.

It seemed possible that the 225 mAb could be inhibiting the constitutive activity of the Δ2-7 EGFR, thus partially explaining its apparent lack of biological activity. To explore this question, we treated both control cells and cells expressing high levels of Δ2-7 EGFR with either EGF or 225 mAb. The Δ2-7 and WT EGFR were sequentially immunoprecipitated, separated by gel electrophoresis and their phosphotyrosine content were evaluated by western blot analysis. As shown in Fig. 10, the anti-Δ2-7 antibody selectively immunoprecipitated the mutant receptor. The small band seen in the WT cells treated with 225 mAb is due to immunoprecipitation via the prebound 225 mAb. Western blots using the anti-PY antibodies demonstrates that the Δ2-7 receptors indeed have constitutive kinase activity and that this activity is not affected by 225 mAb treatment. As expected, the WT EGFR only showed significant PY content in the presence of EGF. These results show that 225 mAb does not affect the activity of the Δ2-7 EGFR and thus its ability to block growth of cells expressing the Δ2-7 EGFR must be due to its inhibition of the WT EGFR. Thus the Δ2-7 EGFR does not behave as a ligand activated EGFR.

Although the Δ2-7 EGFR does not support proliferation of HMEC, perhaps it can stimulate other EGFR-mediated responses, such as cell migration. To test for this possibility, we evaluated the ability of cells to migrate into a "wound" scraped into a cell monolayer. The wound healing assay was done with cells maintained in the presence or absence of 12.5 ng/ml EGF (the maintenance amount in DFCI-1 medium). Prior to initiating the assay, the cells were maintained overnight in the absence of EGF to ensure that all cells started at the same level of

hormonal stimulation. Cells were scraped from the plate with a rubber policeman, the plate rinsed and then fresh medium with or without EGF was added. The initial scraped area was then measured and marked so that the same region could be measured daily. After each measurement additional EGF was added to the +EGF plates in a volume of 1µl/ml of medium to ensure that the ligand did not become depleted.

As shown in Fig. 11, cells expressing secreted EGF had high rates of migration regardless of EGF addition. In contrast, the parental cells showed little movement when EGF was absent and slightly less migration than sEGF cells when EGF was present. The distance migrated by the Δ2-7 EGFR clones was inversely proportional to the level of mutant receptor expressed by the cells. Thus, the clone expressing the highest number of Δ2-7 EGFR moved the least when EGF was added. This observation supports the idea that the Δ2-7 EGF-R in these cells makes the cells less responsive to EGF.

In a recent paper about receptor chimeras (38) the authors report that the adaptor protein SHC is required to produce a motility response in their transfected cells. We therefore decided to examine whether there was an alteration in SHC levels in our cells and determine whether SHC is able to interact with either the endogenous or mutant receptor.

As shown in Fig. 12, the total level of SHC in the parental cells and the Δ2-7 EGFR transductants is quite similar (only the cells expressing secreted EGF seem to have higher levels). When SHC is immunoprecipitated from cells, it results in the co-precipitation of both the endogenous and mutant receptor. In contrast to the situation to the cells making secreted EGF (A1E cells), SHC precipitated from cells expressing the Δ2-7 EGFR was not tyrosine phosphorylated (Fig. 12). The addition of EGF to cells facilitated both association of the EGFR with SHC as well as its tyrosine phosphorylation.

The constitutive association of SHC with the Δ2-7 EGFR is probably due to its constitutive phosphorylation. However, it appears that the associated SHC is not in turn phosphorylated by the Δ2-7 EGFR. Perhaps this leads to the sequestration of this molecule in these cells resulting in a lowered response to ligand. This could result in partial cell "blindness" to its extracellular environment and perhaps explain the oncogenic potential of the Δ2-7 EGFR. Additional experiments are currently underway to test this possibility.

TASK 3: Express genetically altered EGF receptors in mammary epithelial cells

We have examined a variety of different expression vectors for their ability to lead to high level expression in HMEC. In addition, we have also looked at different transfection methods to determine which is optimal.

Materials and Methods

Three different promoters - RSV, SV40 and CMV were tested by insertion of the luciferase gene into their respective plasmids (Rep9, pX - a derivative of pBR322 and pcDNA3, respectively). Two different transfection protocols were also employed as well as three different HMEC cell lines. The cells were transiently transfected by either $CaPO_4$ precipitation or by use of DoTap lipofectamine reagent (Boehringer Mannheim). The choice of DoTap was made through personal communication with Kimberley Spancake in the laboratory of Raymond White.

Cells were transfected overnight using 20 µg DNA/100 mm plate and then incubated in fresh medium lacking the transfection reagents for 24-48 h. They were then solubilized and the amount of luciferase activity in the supernatant determined using a luminometer.

Results and Discussion

With respect to plasmid vectors, optimal transfection efficiency was achieved with the CMV promoter and HMEC 184A1L5. Owing to these results, we have utilized the pcDNA3 plasmid to construct our mutant receptors and have transfected HMEC 184A1L5 with DoTap. We have also inserted the first plasmid of the tetracyclin-responsive 2-plasmid system into these cells using our optimized transfection protocol. We have made these cell lines available to other investigators studying breast cancer.

After several years of attempting to use standard plasmid transfer in HMEC, we have concluded that only retrovirus transduction is suitable for generation of stable cell lines. Although CMV vectors are suitable for transient studies, we have been unable to generate stable cell lines this way. In addition, DoTap only results in transfection of a small percentage (<2%) of the cell population. In contrast, retrovirus containing either EGF receptors or ligands are very efficiently expressed in HMEC, resulting in stable, homogeneous cell populations. Instead of presenting all of the appropriate preliminary data in this section, we have chosen to instead present final data obtained from these transductions (see Tasks 2 & 4).

Different mutant EGF receptors will be constructed Work is in progress on the construction of mutant EGF-R for insertion into retrovirus vectors. In order to differentiate between the modified receptor and the endogenous receptor, we have chosen to include a FLAG marker epitope on the receptors so that they can all be recognized by a single antibody. FLAG is an octapeptide that will be inserted into the EGF-R DNA sequence such that it will replace the epitope used by N13 - a polyclonal anti-EGFR antibody. In this manner we will be able to follow both the endogenous and modified receptor using two, monospecific antibodies.

Replacement of the endogenous receptors with mutant receptors is also being pursued using the chicken EGFR (cEGFR) as the replacement receptor. Inactivation of the endogenous receptor will be accomplished using antagonistic mAb 225. We have obtained the cEGFR and have modified the 5′ and 3′ flanking regions to make them suitable for insertion into a retrovirus vector.

Primers have been constructed to flank the N13 epitope region in the amino terminus of the EGF-R. They have been designed to be complementary for the EGF-R over 24 bp and to be complementary to each other over 24 bp. These flag primers along with the wild-type EGF-R template and two additional primers that flank a region of DNA of about 800 bp are used to amplify the desired piece of DNA. Amplification is done using an air thermocycler. The resulting modified DNA is then cut with Xba1 and Sma1 and inserted into the original EGF-R DNA that has also been cut with the same enzymes to remove the equivalent unmodified piece of DNA. The appropriate DNA pieces are gel purified and then ligated to produce the flag label. Once this tagged, full length DNA is constructed we can either use it to produce further mutants or we can just insert the flag epitope into mutants that have already been constructed. Since the FLAG tag will be on an easily inserted DNA cassette, we can use it for all of the mutant receptors that we plan to examine.

Mutant genes will be transfected into the HMEC and stable colonies will be established We have HMEC clones that contain modified forms of EGF and the Δ2-7 EGF-R. We have not yet isolated other HMEC clones because we have not yet completed the construction of the other EGF-R mutants (also see below).

Task 4: Demonstrate That Mis-sorting or Inappropriate Expression of the EGF Receptor or its

Ligands Provides a Growth Advantage to Normally Organized Epithelial Cells

We are taking two basic approaches to this task. To mis-sort the EGFR, we either have to use a dominant-negative receptor construct or to inactivate the endogenous receptor and replace it with a mutant (mis-sorted) receptor. Because HMEC absolutely require activated EGFR for growth, inactivation of endogenous receptors must be done following expression of the mutant receptor. We have constructed several putative dominant-negative EGFR and expressed them in several model fibroblast cells. These experiments are at a preliminary stage and it is thus inappropriate to describe them in detail. However, we have obtained promising results with dominant negative mutants that can block lysosomal targeting of wild type receptors. This results in the accumulation of the wild type receptors in a currently unidentified cellular compartment. We should be in a position to express these dominant-negative EGFR within the next year.

Replacement of the endogenous receptors with mutant receptors is being pursued using the chicken EGFR (cEGFR) as the replacement receptor. Inactivation of the endogenous receptor will be accomplished using antagonistic mAb 225. We have obtained the cEGFR and have modified the 5′ and 3′ flanking regions to make them suitable for insertion into a retrovirus vector.

We have initiated a major project to modify EGF ligands to understand the role of their spatial distribution in autocrine signaling. All the EGFR ligands consist of a conserved receptor-binding core domain flanked on the carboxy side by a transmembrane domain and on the amino side by a highly variable extension. Some of these extensions are proteolytically removed prior to release of the ligand, such as the case with TGFα. In other cases, such as with heparin-binding EGF, most of the amino-terminus is retained, allowing the ligand to bind to the extracellular matrix or to other cell surface molecules. This extra-receptor binding can have profound effects on cell responsiveness in vitro and presumably in the intact animal. The transmembrane and cytoplasmic domains of the different ligands are also diverse which may indicate specificity in cellular transport, localization or proteolytic release. If the flanking regions of the core binding domain of the EGFR ligands dictate biological activity by controlling ligand distribution and presentation, then what cellular activities depend on these aspects of the ligands?

Understanding the role of ligand distribution is complicated by the fact that most cells making EGFR ligands also express the EGFR and are thus autocrine cells. It is easier to envision a role for ligand presentation in the case of paracrine signaling because of the constraints that the extracellular environment could place on productive signaling. If a cell can bind its own ligands, as in the case with autocrine signaling, then is its distribution or its method of presentation important?

Because all EGFR ligands are synthesized as membrane-bound precursors, we first explored the role played by the transmembrane anchoring domain. We made two derivative of EGF: one lacking and one possessing a membrane anchoring region. Both constructs lacked the normal amino-terminus extension to simplify the analysis. These artificial EGFR ligands were then expressed in 184A1 HMEC to determine how they affected cell behavior. Surprisingly, we found that removal of the transmembrane domain resulted in a non-interruptible autocrine loop, apparently through an intracrine mechanism. Significantly, these cells could not create organotypic structures when grown on matrigel. Our results suggest that the spatially restricted release of EGFR ligands, mediated by the transmembrane domain, is important in

normal tissue organization.

Materials And Methods

General -- Monoclonal antibody 225 (mAb 225) directed against the EGFR was isolated from a hybridoma cell line obtained from the American Type Culture Collection. Monoclonal HA directed against EGF was a kind gift from Katsuzo Nishikawa of the Kanazawa Medical University in Japan. Recombinant EGF (QBC,Inc) was conjugated to Keyhole limpet hemocyanin (KLH;Pierce) using sulfo-MBS (Pierce) after first introducing a sulfhydryl group using Traut's Reagent (Pierce) according to manufacture's instruction The KLH-EGF conjugate was used as an antigen to produce rabbit antisera. Vector pEGF-1 containing the mature sequence of human EGF was a gift from Salil Niyogi. Cells were counted using a Coulter Counter.

Construction of sEGF -- An artificial secreted form of human EGF (sEGF) was constructed using the DNA sequence of human EGF that was originally chemically synthesized fused to 200 bp fragment of the 5' untranslated region and adjacent signal sequence of the EGFR. The EGF DNA was removed from pEGF-1 by digesting with EagI, endfilling with Klenow, and digesting with EcoRI. The EGF DNA was ligated to pBluescript (Stratagene) that was digested with HindIII, endfilled with Klenow and digested with EcoRI to create pBluescript-EGF. The 5'-untranslated region and signal sequence of the EGFR were isolated using Polymerase Chain Reaction(PCR) with primers to the SP6 promoter (5'-GTATTCTATAGTGTCACCTA-3') and the EGFR signal sequence ('5-GCCCGACTCGCCGGGCAGAG-3') using pLOLB (55) as the template. The PCR product was digested with XbaI to remove unwanted vector sequences, resulting in an insert with a 5' XbaI end and a single 3' A-overhang left by the Taq polymerase. This insert was ligated into pBluescript-EGF that was first digested with EcoRI and endfilled with Klenow followed by addition of T-overhangs with Taq polymerase and digestion with XbaI.

For insertion into the MFG retrovirus vector, StyI and BglII sites were made at the 5' and 3' end of the sEGF construct using the primers '5-CTT CGG GGA GCA GCC ATG GGA CCC TCC G-3' and '5-AGA TCT AAC GGA GCT CCC ACC ACT-3' . This set amplified the entire sEGF gene with the appropriate new restriction sites. The product was then ligated into pBluscript following digestion with SmaI and addition of T-overhangs with Taq polymerase. The same protocol was followed for the EGF-Ct construct except that a compatible NcoI site was used instead of the StyI site using the primer pair 5'-CCA TGG GAC CCT CCG GGA CG-3' and '5-AGA TCT ACT GAG TCA GCT CC-3'. In brief, the PCR reaction mixture included 100pmol of each primer, 20ng of temple, 200μM of each dNTP, 25mM $MgCl_2$ and 2.5 U of Taq polymerse. A DNA thermal cycler (Perkin Elmer Cetus) was used for 25 cycles with an annealing temperature at 50°C. Final products were confirmed by DNA sequencing.

The PCR product was isolated after digestion with BspH1 and BamH1 and inserted into the Nco1 / BamH1 sites of the retroviral vector, MFG. The fidelity of the insert was verified by DNA sequencing. To generate a virus producing cell line, MFG-*EGF* and MFG-*ctEGF* plasmid DNA was transfected into the Y-CRIP packaging cell line (originally obtained from R. Mulligan, Whitehead Institute of Biomedical Research, Cambridge, MA).

Cells were transfected with retrovirus stock using polybrene and grown for 2 days before plating at clonal density in medium lacking EGF. Individual colonies were isolated using cloning rings and then screened by immunofluorescence and by measuring the medium for

the presence of EGF as described below. All experiments were done with several independently isolated colonies.

Measurement of sEGF in media - A sandwich ELISA was developed to measure sEGF levels in the medium. High binding ELISA plates (Corning) were coated with 50 µl of monoclonal antibody HA against EGF (5-10 µg/ml) diluted in phosphate-buffered saline pH 7.4 with 0.02% sodium azide (PBSN). The plates were rinsed 4 times with wash buffer (0.05% Tween-20 in PBSN) before each new addition The plates were then blocked using blocking buffer (10% horse sera in PBSN). Human recombinant EGF was diluted in blocking buffer for a standard curve ranging from 3 to 100 pg. A rabbit polyclonal sera directed against EGF was used as a secondary antibody diluted 1:100 in blocking buffer. Alkaline phosphatase-conjugated goat anti-rabbit antibody (Sigma) was used as the tertiary antibody at a dilution of 1:6000. The ELISA was developed by rinsing the plates twice with 10mM diethanolamine, 0.5 mM $MgCl_2$, pH 9.5 and then adding 50µl of 1mg/ml dinitrophenol (Sigma) dissolved in the same buffer. The reaction was allowed to go for 4-10 minutes and then quenched with 0.1M EDTA. The ELISA plates were read at 405mn using a microplate reader.

Results and Discussion - The structure of the two EGF constructs we expressed in HMEC is shown below in Fig. 13.

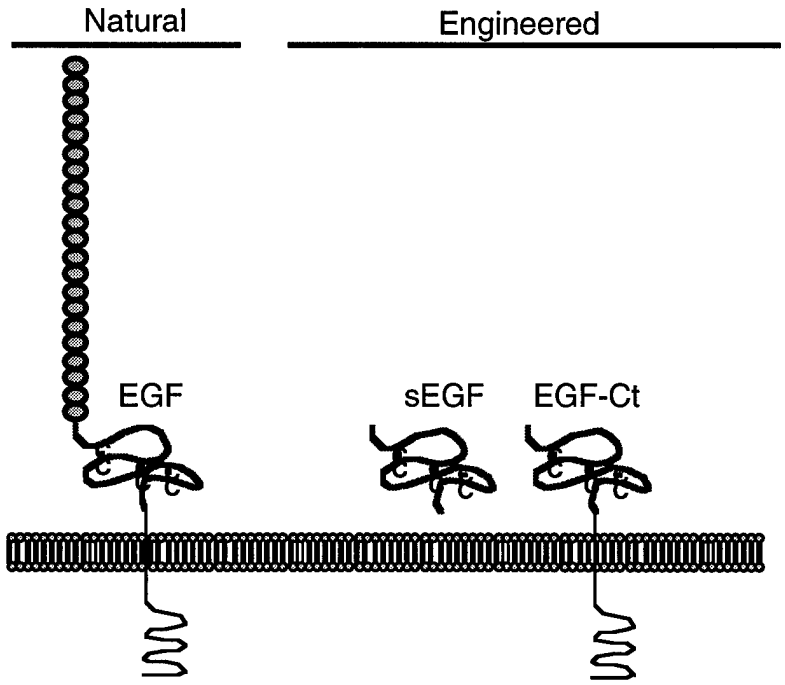

Figure 13. Structure of EGF and engineered ligands. Natural EGF (left) is made as a transmembrane precursor. We modified the natural gene by removing the transmembrane and amino-terminus extention to make sEGF. Adding back the transmembrane carboxy-terminus gave rise to ct-EGF and adding back the amino-terminus gave rise to at-EGF. All constructs use the signal sequence from the EGFR.

After transduction of HMEC with retrovirus containing the two genes, we picked random clones and evaluated them for the level of EGF expression by a sensitive EGF ELISA assay. This was done in the presence and absence of 225 mAb to prevent utilization of the EGF by the endogenous HMEC EGFR. As shown in Fig. 14, several of these clones secreted very high levels of EGF into the medium. The presence of the anti-EGFR antibody 225 resulted in a substantial increase in levels of EGF found in the medium. We conclude that both sEGF and EGF-Ct are efficiently made by HMEC and are secreted at similar levels.

The distribution of both EGFR and EGF was then evaluated by immunofluorescence. As shown in Fig. 15, the EGFR displays primarily a surface distribution in the parent, WT cells. As expected, endogenous levels of EGF were insignificant. Cells expressing either sEGF or EGF-Ct displayed a significantly different distribution of the EGFR, the receptor being primarily found into an intracellular compartment. This redistribution of the EGFR is identical as that found following treatment with exogenous EGF (data not shown). This indicates that the EGF made by the cells was down-regulating the EGFR. EGF staining in cells expressing EGF-Ct was primarily localized at the cell surface, but could also be found in vesicles co-localizing with internalized EGFR. Staining of EGF was faint for cells expressing sEGF. When the signal was amplified, as shown in Fig. 16, the EGF could be found co-localized in EGF-R containing vesicles.

To determine the effect of sEGF and EGF-Ct on growth of HMEC, cells were plated out at clonal density in the presence and absence of exogenous EGF and the antagonistic anti-EGFR antibody 225. After 3 weeks growth, plates were stained with crystal violet to visualize the cells. As shown in Fig. 17, EGF had a positive effect on the growth of the parent (WT) cells whereas the 225 mAb completely blocked cell growth. Cells expressing either sEGF or EGF-Ct grew equally well in the presence or absence of exogenous EGF. However, although the growth of cells expressing EGF-Ct could be blocked with the 225 mAb, cells expressing sEGF were not affected. These results indicate that removal of the transmembrane domain of EGF results in a non-interruptible, or "short-circuit" autocrine loop.

To examine these results in more detail, we examined both growth rates and phosphorylation of the EGFR substrate SHC in cells expressing sEGF or EGF-Ct. As shown in Fig. 18A, The growth rate of the parent HMEC was positively affected by the addition of EGF and negatively affected by the addition of 225 mAb. The cells expressing sEGF were not affected by either EGF or 225 whereas cells expressing EGF-Ct could be inhibited by 225 mAb. Similarly, the addition of EGF to the parent cells was required to observe significant SHC phosphorylation whereas EGF addition had little affect on SHC phosphorylation in cells expressing either sEGF or EGF-Ct. Significantly, 225 mAb was able to block SHC phosphorylation only in the case of cells expressing EGF-Ct. These data indicate that the 225 mAb is unable to block EGFR activation when the EGF made by the cells lacks a transmembrane domain.

Because the autocrine loop in cells making sEGF cannot be interrupted by the addition of exogenous antibodies, this suggests that the EGFR is occupied prior to arrival at the cell surface, perhaps during receptor recycling or synthesis. If the autocrine loops cannot be interrupted, then any spatial information that the cells obtain from the selective interruption of these loops must be lost. To determine whether HMEC obtain significant spatial information from EGFR autocrine signaling, we examined the ability of cells expressing sEGF or EGF-Ct to organize on Matrigel. As shown in Fig. 19, the WT cells only organize well in the presence of EGF. Organization on Matrigel requires significant cell motility as well as cell-to-cell interactions. Exogenous EGF is probably required to stimulate cell motility. Consistent with this explanation, cells can organize in the absence of exogenous EGF when plated at a sufficiently high density (data not shown).

Cells expressing EGF-Ct could organize in the absence of exogenous EGF, but were blocked by the addition of 225 mAb. However, cells expressing sEGF did not organize in either the presence of EGF or 225 mAb (Fig. 19). Instead, they formed spherical clumps of cells. These data indicate that the ability to form tubular/ductal structures requires the correct pattern of

interruption of EGFR autocrine loops. Thus the spatial pattern of EGF/EGFR interactions is an important component of normal organization of HMEC.

Task 5: Determine how the pattern of spatial regulation of the EGFR affects its ability to transactivate and transmodulate erbB-2

We have previously investigated the mechanisms that regulate the activity and distribution of EGF-R in cells. We have now extended our studies to examine the ability of the EGF-R to transmodulate erbB-2. We report here that activation of the EGF-R results in the tyrosine phosphorylation of erbB-2 and a subsequent loss in the cellular mass of erbB-2. Surprisingly, this transmodulation does not require either the intrinsic tyrosine kinase activity of the EGF-R or sequences in its regulatory carboxy tail. Sequences containing the lysosomal targeting domain of the EGF-R were required, however, suggesting that correct intracellular trafficking of the EGF-R is necessary for transmodulation of other members of the erbB family.

Materials and Methods

General - Polyclonal rabbit antibody N13 directed against a peptide corresponding to residues 1-13 in human EGF-R was a gift of Dr. Debora Cadena. Polyclonal rabbit antibody 1917 to erbB-2 directed against a peptide corresponding to the 18 carboxy terminal residues of human erbB-2, were provided by Dr. Gordon Gill. Rabbit polyclonal antibody C18 against amino acids 1169-1186 of neu/erbB-2 was obtained from Santa Cruz Biotechnology. Polyclonal rabbit antibodies specific for phosphotyrosine were generated and affinity-purified as described (56). Monoclonal antibodies 528, 579,and 225 against the EGF-R (54) were purified from hybridomas obtained from the American Type Culture Collection. Monoclonal antibody 13A9 against the human EGF-R was a generous gift from Genentech. Ab5 against the excellular domain of human erbB-2 was obtained from Oncogene Sciences. Secondary antibodies labeled with either Texas Red or fluorescein were obtained from Cappel laboratories.

Cell Culture - B82 mouse L cells, which contain no endogenous EGF receptors (57), and B82 cells transfected with normal (WT) or mutated (M^{721}, c'647, c'958, and M^{721}c'958) human EGF receptors were a generous gift of Dr. Gordon Gill. Their construction was described previously (58). B82 cells were grown in Dulbecco's modified Eagle's medium (DME, Flow Laboratories) containing dialyzed 10% calf serum (HyClone). 5 μM methotrexate was added to the medium for those cells transfected with human EGF receptor. The human mammary epithelial cell line 184A1L5 (59) was obtained from Dr. Martha Stampfer and was cultured in medium DFCI-1 as described (60). The human mammary epithelial line HB2 was a gift from Joyce Taylor-Papadimitriou and were grown as described (61). SKBR3 cells (62) were obtained from the American Type Culture Collection and grown in McCoys 5A supplemented with 10% fetal calf serum (HyClone).

Quantification of EGF-R , erbB-2 and phosphotyrosine levels - Confluent cultures of cells were rinsed and lysed in an NP-40 buffer (150mM NaCl, 1% NP-40, 50mM Tris pH 8) and debris removed by centrifugation. Samples were brought to 2% SDS, 1% β-mercaptoethanol and heated to 100°C for 5 min. Equal amounts of total cellular protein from each sample were separated on 5-7.5% gradient gels and transferred to nitrocellulose. EGF-R and erbB-2 were detected by N-13 and 1917 polyclonal antisera respectively using ^{125}I-labeled protein A as described (63). The concentrations of and incubation times with ^{125}I-labeled protein A were chosen to be in the linear range of the protein load of the gels. The blots were analyzed by storage phosphor plates using the Bio-Rad G250 Molecular Imager. The Bio-Rad Molecular

Analyst package was used to quantify the amount of radioactivity associated with each band. In some cases, EGF-R levels were determined by a sandwich ELISA as previously described (64). In this case, cells were extracted for 10 min at 0°C in 20 mM CHAPS, 10 mM HEPES buffer (pH 7.4), 4 mM iodoacetate and 100μg/ml each of leupeptin, chymostatin, pepstatin and aprotinin. Standard curves were generated using extracts from B82 cells expressing a known level of EGF-R protein and using receptor-negative B82 cells as blanks.

To determine the tyrosine phosphosphate content of erbB-2 protein, cells were lysed for 10 min at 0°C in 1% Triton X-100, 150 mM NaCl, 50 mM Hepes (pH 7.2), 10% glycerol, 1 mM Na_3VO_4, 4 mM iodoacetate and 10μg/ml each of chymostatin, pepstatin, leupeptin and aprotinin. After centrifugation for 10 min at 10,000 x g at 0°C, the 1917 anti-erbB-2 polyclonal antiserum was added (1:100) followed by rocking for 3 h followed by the addition of 100 μl of protein A sepharose (50% slurry) for an additional hour. The beads were washed several times in lysis buffer and boiled in SDS sample buffer prior to gel electorphoresis and transfer to nitrocellulose as detailed above. Phosphotyrosine was detected using affinity-purified polyclonal antibodies and erbB-2 protein was quantified in a parallel blot using 1917 antiserum. The Bio-Rad G250 Molecular Imager and the Molecular Analyst package was used to quantify the amount of radioactivity associated with each band.

Quantification of EGF-R mRNA levels- Total cellular RNA was isolated using Tri-Reagent (Molecular Research Center, Inc.) following the manufacture's directions. cDNA was synthesized using M-MLV Reverse Transcriptase (Promega) and specific products were amplified by PCR using the Idaho Technology air cycler with the following primers and protocols; erbB2 - 5' AACTGCACCCACTCCTGTGT 3' and 5' CAGGGATCCAGATGCCCTTG 3' at 63° annealing, 94° polymerization for 15 s for 30 cycles. G3PDH - 5' GAGCTTGACAAAGTGGTCGTTGAGG 3' and 5' CCACAGTCCATGCCATCACTGCCAC 3' at 63° annealing, 94° polymerization for 15 s for 24 cycles. The number of cycles was chosen empirically to keep product amplification in the linear range. Reaction products were separated on 1.8% agarose gels and stained with ethidium bromide.

Fluorescence Microscopy- - Cells were plated on fibronectin-coated coverslips 48 hrs before the experiment. Cells treated either without or with EGF were fixed for 10 min with freshly prepared 3.6% paraformaldehyde and 0.024% saponin in Ca^{2+}, Mg^{2+}-free phosphate buffered saline. Free aldehyde groups were quenched with 0.1% $NaBH_4$ for 10 min. Cells were incubated simultaneously with a mixture of anti-EGF-R monoclonals 528, 579, 225 and 13A9 (10μg/ml each) and anti-erbB-2 C18 (1:100; Santa Cruz Biotechnology, Inc.) in 0.012% saponin for 45 min followed by staining with FITC-labeled goat anti-mouse and Texas Red-labeled goat anti-rabbit IgG antibodies (1:100) for 45 min. The coverslips were mounted in ProLong antifade medium (Molecular Probes, Inc.) and viewed with a Nikon inverted fluorescence microscope with a 40x oil immersion objective. Images (512x512) were acquired using a Photometrics cooled CCD camera with a Macintosh workstation running OncorImage software. For confocal microscopy, samples were viewed with a Bio-Rad MRC 600 laser scanning confocal imaging system attached to a Zeiss Axioplan microscope with a 60X objective. Excitation was achieved with a Krypton/Argon laser using the 488 and 568 nm lines. Paired images (384x512 pixels each) were individually scaled to 256 gray levels using Adobe Photoshop 3.0 on the Macintosh before output to a film recorder.

Flow cytometry - - Cells were removed from plates by a brief trypsinization, which did not alter the measurable number of either EGF-R or erbB-2 at the cell surface. Cells were fixed for 10

min at 22°C in freshly prepared 3.6% paraformaldehyde, rinsed and incubated for 1 h in either anti-EGF-R mAb 225 or anti-erbB-2 mAb Ab5 followed by FITC-labeled goat-anti-mouse antibody for 1 h. Samples were analyzed on a FACScan flow cytometry instrument (Becton-Dickinson, Mountain View, CA) and the data analyzed using Cell Quest software

Results and Discussion

EGF treatment reduces erbB-2 levels in human mammary epithelial cells It is known that binding of EGF to its receptor leads to rapid internalization and reduction of EGF-R levels as a result of lysosomal targeting (65). It is also well established that activated EGF-R can form heterodimers with erbB-2, resulting in erbB-2 transactivation (66). Studies using a normal mouse mammary cell line, HC11, showed that EGF treatment resulted in a loss of erbB-2 cell surface expression due to accelerated degradation (52). Other studies, however, using either Rat-1 cells (67) or transformed human cell lines showed that EGF had no affect on erbB-2 levels (62). Our first goal, therefore, was to determine whether erbB-2 expression or trafficking was affected by EGF in a non-transformed human mammary epithelial cell line, 184A1L5 (59). This line is mitogenically responsive to EGF and expresses both EGF-R and erbB-2.

Cells were treated with 100 ng/ml of EGF for 1 h at 37°C. The levels of cell surface EGF-R and erbB-2 were then measured by flow cytometry. As shown in Figure 20, EGF treatment reduced the surface expression of EGF-R in 184A1L5 cells by approximately 50%. Although cell surface erbB-2 levels were not as high as EGF-R levels, EGF treatment resulted in an approximately 3-fold reduction in their levels. These data demonstrate that activation of the EGF-R in mammary epithelial cells not only downregulates the EGF-R, but also reduces the surface levels of erbB-2.

To determine whether the reduction of surface erbB-2 levels was accompanied by a reduction in total cellular erbB-2 mass, we treated cells with EGF for varying periods of time and then determined total erbB-2 levels by western blot analysis. EGF-R levels were simultaneously measured by using a specific ELISA (64). EGF treatment resulted in a progressive loss of both proteins over a 24 hour time period (Fig. 21, left panel). These data show that EGF can downregulate erbB-2 levels in cells in a similar manner as the EGF-R, confirming results previously obtained with mouse mammary epithelial cells (52). The kinetics and extent of loss of both proteins were remarkably similar, suggesting that a similar mechanism may be responsible. If this 'transmodulation' of erbB-2 by the EGF-R requires a direct physical interaction between the two molecules, then it should be possible to define the responsible structural features of the EGF-R.

Model system for analyzing erbB-2 transmodulation To define the structural features of the EGF-R responsible for transmodulation of erbB-2, it is preferable to use a cell type which expressed normal levels of erbB-2, but does not have endogenous EGF-R. This allows the use of different mutant forms of the EGF-R introduced by gene transfection. A suitable cell type is the mouse B82 cell line which expresses the murine homolog of erbB-2, but lacks endogenous EGF-R (57). To determine whether activated EGF-R could alter the levels of erbB-2 in this cell line, we added EGF to B82 cells expressing an introduced human EGF-R (58). As shown in Fig. 21 (right panel), EGF treatment caused an approximate 75% loss of both EGF-R and erbB-2 protein levels. Again, the kinetics and extent of erbB-2 loss paralleled that observed for the EGF-R. We conclude that the ability of the EGF-R to affect the cellular levels of erbB-2 in B82 cells appears similar to that observed in human mammary epithelial cells.

The rapidity of the EGF-induced loss of erbB-2 implicates a degradative mechanism. It remained a formal possibility, however, that a reduction in erbB-2 mRNA levels could also be involved. To check for this possibility, both 184A1L5 and B82 cells were treated without or with 100 ng EGF for 4 h at 37°C. Total RNA was extracted and the levels of erbB-2 mRNA were determined by RT-PCR. As shown in Fig. 22, treatment of either cell type with EGF had no discernible effect of erbB-2 mRNA levels. This result is consistent with a posttranslational mechanism for the reduction of erbB-2 levels by EGF treatment.

Decreased levels of erbB-2 in response to EGF is due to enhanced lysosomal targeting It is known that the decrease in EGF-R protein levels in response to EGF addition is due to enhanced lysosomal targeting. Because of the similar kinetics of the loss of both EGF-R and erbB-2, it seemed reasonable that the same mechanism could be responsible. Immunofluorescence visualization is a sensitive method for determining enhanced lysosomal targeting of EGF-R. Therefore, we visualized the distribution of both EGF-R and erbB-2 in B82 cells incubated either with or without EGF.

As shown in Fig. 23A, EGF-R display a predominantly cell surface localization in the absence of EGF. Surprisingly, erbB-2 was primarily localized in small cytoplasmic vesicles, although some was found associated with the cell surface (Fig. 23B). There was little overlap between the EGF-R and erbB-2 staining pattern. The addition of peptide specific for the anti-erbB-2 antibody abolished the erbB-2 immunofluorescence, but had no effect on the EGF-R staining pattern (Fig. 23C and 23D), indicating the observed localization was specific for erbB-2. The addition of EGF resulted in reduced levels of surface EGF-R and a corresponding increase in intracellular EGF-R, particularly in perinuclear and lysosomal structures (Fig. 23E). Significantly, EGF also caused a redistribution of erbB-2 into lysosomal structures (Fig. 23F). Although EGF treatment increased the overlap between intracellular EGF-R and erbB-2, there was still a large number of vesicles that contained either EGF-R or erbB-2, but not both. We conclude that EGF treatment accelerates lysosomal targeting of both the EGF-R and erbB-2, but that the normal cellular distribution of the two proteins is different.

We were surprised at the predominant intracellular localization of erbB-2 because this receptor has previously been described as being cell surface-associated (67). To determine whether the intracellular localization of erbB-2 in B82 cells was atypical, we used confocal microscopy to examine the localization of erbB-2 in various cell lines (Fig. 24). In the case of both B82 cells and the nontransformed human mammary epithelial cell line HB2, there was a high levels of intracellular erbB-2 (top and middle right panels) whereas the EGF-R displayed primarily a cell surface distribution (top and middle left panels). The human mammary epithelial cell line 184A1L5 also displayed significant levels of intracellular erbB-2 (data not shown). In contrast, the transformed cell line SKBR3 which overexpresses erbB-2, showed an almost exclusive cell surface localization (bottom panels). This distribution also corresponded to the location of the EGF-R (bottom left panel). We conclude that a significant fraction of erbB-2 can exist in an intracellular compartment in nontransformed cells and that in the absence of EGF, the distribution of EGF-R and erbB-2 is distinct. The cell surface distribution of erbB-2 previously described may either be a result of cell transformation or overexpression of erbB-2.

Structural aspects of EGF-R required for erbB-2 transmodulation Several models could explain the ability of activated EGF-R to target erbB-2 to lysosomes. One is that the EGF-R activates erbB-2 by direct tyrosine transphosphorylation. The activated erbB-2 would then enter the lysosomal targeting pathway by a similar mechanism as the EGF-R. We tested this possibility

by determining the effect of EGF on erbB-2 levels using cells expressing kinase inactive EGF-R. As shown in Fig. 25, full length kinase inactive EGF-R still reduce erbB-2 levels in response to EGF, although not as rapidly as the wild type EGF-R (6A versus 6B). This suggests that direct tyrosine phosphorylation of erbB-2 by the EGF-R is not necessary for erbB-2 transmodulation.

Heterodimerization between EGF-R and erbB-2 is thought to occur through their extracellular domains, but transactivation may also require cytoplasmic sequences of the EGF-R (68-69). These sequences fall into three main domains: the regulatory cytoplasmic tail (residues 958-1186), the conserved kinase domain (688-958) and the submembrane region (residues 645-688). In an effort to determine which domain may be involved in transmodulation of erbB-2, we used B82 cells expressing EGF-R that lacked various regions. As shown in Fig. 25B, receptors lacking all cytoplasmic sequences (c'647) or sequences distal to the submembrane region (c'688) did not reduce erbB-2 levels following EGF addition. Receptors having the conserved kinase domain (c'958) were able to efficiently reduce erbB-2 levels in response to EGF as effectively as full length receptors (Fig. 25A). Eliminating the intrinsic kinase activity of the c'958 receptor through a point mutation in its ATP binding site (M^{721}) also did not eliminate its ability to reduce erbB-2 levels (Fig. 25B). We conclude that although the kinase domain of the EGF-R is required for transmodulation of erbB-2, the kinase activity of this domain is not required. This suggests that direct phosphorylation of erbB-2 by the EGF-R is not necessary.

The ability of mutant EGF-R's to induce tyrosine phosphorylation of erbB-2 correlates with its ability to transmodulate erbB-2 levels Although direct phosphorylation of erbB-2 by occupied EGF-R is clearly not involved in transmodulation, it seemed possible that heterodimerization of kinase-inactive EGF-R with erbB-2 could result in activation of erbB-2 through interaction of their cytoplasmic regions. It has been previously shown that EGF-R lacking intrinsic kinase activity can activate erbB-2 (70). To test this possibility, we treated cells expressing various EGF-R mutants for 15 and 120 minutes with EGF. ErbB-2 was then immunoprecipitated and probed for phosphotyrosine by western blot analysis. As shown in Fig. 26, both the full length and c'958 mutants were able to induce tyrosine phosphorylation of erbB-2. Phosphorylation was highest at 15 min and fell by 2 h. The c'958 EGF-R mutant was able to induce a higher stimulated level of erbB-2 phosphorylation, although the basal level of erbB-2 phosphorylation was higher as well. Interestingly, kinase-inactive versions of the full length and c'958 EGF-R were also able to induce tyrosine phosphorylation of erbB-2, albeit to a lower degree than the kinase active EGF-R. The kinetics of erbB-2 phosphorylation were also similar.

In contrast to the results obtained with the full length and c'958 EGF-R, receptors truncated to residue 688 were not able to induce tyrosine phosphorylation of erbB-2 (Fig. 27). Thus the ability of EGR-R able to mediate phosphorylation of erbB-2 is correlated with its ability to reduce erbB-2 levels. This is consistent with a model in which erbB-2 is transactivated by heterodimerization with the EGF-R. The transactivated erbB-2 would then be targeted to lysosomes in an analogous fashion as ligand-activated EGF-R.

The distal region of the EGF-R tyrosine kinase domain is required for transmodulation of the EGF-R Although the region between 688 and 958 of the EGF-R contains the conserved tyrosine kinase domain, another activity that has been mapped to the distal region of this domain is endosomal retention/lysosomal targeting (between 899 and 958) (63). To determine whether this region is required for transmodulation of erbB-2, we prepared an EGF-R truncated at residue 899. As shown in Fig.28, the c'899 EGF-R was unable to mediate a reduction of erbB-2 levels in response to EGF. In addition, no tyrosine phosphorylation of erbB-2 was observed.

We conclude that the region of the EGF-R that contains the endosomal retention/lysosomal targeting sequences also contain the sequences necessary for both transactivation and transmodulation of erbB-2.

Over the last several years, it has become clear that the members of the EGF receptor family interact extensively. These interactions are thought to be important in generating the pattern of intracellular signals triggered by ligand binding (45). Receptor activity is regulated by diverse dynamic processes, such as phosphorylation, endocytosis and lysosomal targeting and these processes require specific receptor sequences that interact with regulatory machinery of the cell. Previously, we have identified EGF receptor sequences that are required for its endocytosis and lysosomal targeting (63). In the current study, we sought to define EGF receptor domains that are responsible for interacting with erbB-2. We examined changes in erbB-2 phosphorylation and protein levels because these parameters are fairly direct measurments of the status of erbB-2 itself. In addition, these parameters reflect the status of the entire cellular pool of erbB-2.

We found that transmodulation of erbB-2 by EGF is fairly rapid, occurring with similar kinetics and extent to that observed for downregulation of the EGF-R. Analysis of EGF-R mutants demonstrated that neither intrinsic tyrosine kinase activity nor the regulatory carboxy-terminus distal to the kinase domain were required for reduction of erbB-2 levels. Further truncation of 59 amino acids from the carboxy end of the kinase domain of the EGF-R eliminated transmodulation as did further receptor truncations. The simplest intrepretation of this data is that are sequences between 899 and 958 of the EGF-R are required for downregulation of erbB-2.

Because tyrosine phosphorylation of erbB-2 always accompanied its downregulation, it appears likely that activation of erbB-2 signaling is also occurring. It was surprising, however, that EGF-R kinase activity was not required for EGF-induced erbB-2 phosphorylation. This implies that at least a degree of erbB-2 phosphorylation is not through direct transphosphorylation by the EGF-R. One possible mechanism is that EGF-R/erbB-2 heterodimerization induces a conformational change in erbB-2 that activates its intrinsic kinase activity. This mode of receptor phosphorylation would be analogous to transactivation of erbB-2 by heregulin-activated erbB-3. ErbB-3 is reported to have impaired kinase activity, yet retains the ability to heterodimerize and lead to tyrosine phosphorylation of erbB-2 (71). Activation of erbB-2 by heterodimerization with kinase-inactive EGF-R has previously been demonstrated (70). It has also been suggested that erbB-2 can tyrosine phosphorylate kinase inactive EGF-R following EGF treatment (68). The higher level of erbB-2 phosphorylation elicited by the kinase active receptor, however, indicates that erbB-2 could also undergo direct transphosphorylation if its heterodimer partner possesses kinase activity.

There is no obvious direct relationship between the degree of erbB-2 phosphorylation and its downregulation (Fig. 25 and 26). However, this does not mean the phosphorylation per se is not required for erbB-2 downregulation. The degree of phosphorylation seen in our experiments may reflect modification of multiple tyrosine residues in erbB-2, not all of which may be involved in receptor trafficking. This is especially plausible if the different EGF-R mutants which transmodulate erbB-2 vary in their ability to induce phosphorylation by transphosphorylation versus transactivation. However, levels of erbB-2 phosphorylation drop from a peak at 15 min to a lower, more uniform value for all EGF-R mutants tested(Fig. 26). Because erbB-2 downregulation requires prolonged incubation with EGF, it is difficult know

the relevant time frame to compare these two processes. Finally, there may actually be no direct relationship between phosphorylation and downregulation. Both processes may simply reflect the consequence of EGF-R and erbB-2 interactions. Further studies will be required to discriminate between these possibilities.

Although the extracellular domain of the EGF-R has been reported to be sufficient for heterodimer formation, it is clearly not sufficient to either transactivate or transmodulate erbB-2 (68-69). Because removal of sequences distal to 899 in the conserved kinase domain abolishes erbB-2 transmodulation, an additional cytoplasmic interaction between the two receptors may be required to efficiently heterodimerize or cause an activating conformational change. Alternately, trafficking of the EGF-R into intracellular compartments containing high levels of erbB-2 may be required for heterodimerization, activation and downregulation of erbB-2.

Consistent with a role for EGF-R trafficking in erbB-2 activation is our observation that there are significant intracellular pools of erbB-2 in cells which display EGF-R-mediated transmodulation. In the absence of ligand, there was little overlap of EGF-R and erbB-2 distribution. In the presence of EGF, however, there was significant overlap between the distribution of EGF-R and erbB-2. In addition, the region of the EGF-R required for transmodulation of erbB-2 (between 899-958) maps to the region necessary for lysosomal targeting of the EGF-R. Recently, it has been shown that this domain of the EGF-R binds to the protein SNX1 which mediates receptor transfer to late endosomes and lysosomes (72). Alternately, the region between 899-958 could simply allows heterodimerization of the EGF-R to erbB-2 which would in turn allow transactivation and independent lysosomal targeting.

Despite the significant intracellular pools of erbB-2 that we observed, erbB-2 was also clearly detectable at the cell surface. In addition, EGF treatment reduces the cell surface levels of erbB-2. Because the "internalization defective" EGF-R mutants M^{721} and c'958 were very effective in transmodulating erbB-2, it would appear at first glance that the interactions between EGF-R and erbB-2 are most likely to occur at the cell surface. This may indeed be the case, but the temporal resolution of our experiments is not sufficient to resolve this issue. Although several of our EGF-R mutants are internalization defective, this only referes to their inability to undergo accelerated internalization following receptor occupancy. They still undergo significant internalization as a normal consequence of general membrane turnover and still display occupancy-induced retention within endosomes (63, 73). Indeed, the constitutive internalization rate of 0.02 min^{-1} determined for erbB-2 and internalization defective EGF-R translates to a surface $T_{1/2}$ of 30 min (51, 74). Because this is much faster than the observed kinetics of erbB-2 loss, inhibiting constitutive recycling of erbB-2 would be an effective mechanism for reducing erbB-2 levels. Constitutive endocytosis of "internalization defective" EGF-R mutants therefore occurs at a sufficient rate to allow intracellular heterodimerization and transmodulation on the time scale observed in our experiments. We have previously observed that a fraction of kinase-inactive EGF-R accumulates in intracellular vesicles following EGF addition (74). This may or may not reflect their site of intereaction with erbB-2. Clearly, further studies are needed to identify the compartment in which EGF-R interacts with erbB-2.

Overexpression of erbB-2 is correlated with several cancers, particularly breast cancer (75-76). SKBR3 is a breast cancer cell line that overexpresses erbB-2 (77). Interestingly, these cells show an almost exclusive surface localization of erbB-2 and do not display EGF-induced

downregulation of erbB-2 (62); also data not shown). A correlation between high erbB-2 levels and low transmodulation by the EGF-R has been observed by other investigators as well (78). It is possible that overexpression of erbB-2 saturates the intracellular trafficking machinery, preventing downregulation of erbB-2 following activation. This may enable the cell to exhibit prolonged signalling from erbB-2 and confer a growth advantage, analogous to the situation postulated for internalization-defective EGF-R (4). Alternatively, a modified distribution of EGF-R and erbB-2 may facilitate heteodimerization in compartments that normally would not contain such activated complexes. This in turn may allow access to a different set of substrates or restrict the influence of negative regulatory elements, such as phosphatases or kinases. Further work is obviously necessary to determine the mechanisms and importance of transmodulation of erbB-2 by the EGF-R. It is clear, however, that normal regulation of both EGF-R and erbB-2 requires their correct intracellular trafficking.

Conclusions

We are making excellent progress on our project. It has been appreciated that growth factors provide important information to the cell regarding its environment. They can also stimulate mitogenesis. It has been assumed that their role in cancer relates to their mitogenic potential. Our results indicate that the role of growth factor receptors in environmental sensing is also involved in transformation by preventing the cell from perceiving context. Thus, negative growth signals cannot be seen. This result has important implications in future strategies to understand the mechanisms of cancer progression.

REFERENCES

1. Momburg, F., Moldenhauer, G., Hammerling, G. J., and Moller, P. (1987) *Cancer Res.* **47,** 2883-91
2. Simpson, J. F., and Page, D. L. (1992) *Am. J. Path.* **141,** 285-289
3. Chen, W. S., Lazar, C. S., Lund, K. A., Welsh, J. B., Chang, C. P., Walton, G. M., Der, C. J., Wiley, H. S., Gill, G. N., and Rosenfeld, M. G. (1989) *Cell* **59,** 33-43
4. Wells, A., Welsh, J. B., Lazar, C. S., Wiley, H. S., Gill, G. N., and Rosenfeld, M. G. (1990) *Science* **247,** 962-964
5. Bates, S. E., Valverius, E. M., Ennis, B. W., Bronzert, D. A., Sheridan, J. P., Stampfer, M. R., Mendelsohn, J., Lippman, M. E., and Dickson, R. B. (1990) *Endocrinology* **126,** 596-607
6. Stampfer, M. R., Pan, C. H., Hosoda, J., Bartholomew, J., Mendelsohn, J., and Yaswen, P. (1993) *Exp. Cell Res.* **208,** 175-188.
7. Matthay, M. A., Thiery, J. P., Lafont, F., Stampfer, M. F., and Boyer, B. (1993) *J. Cell Sci.* **106,** 869-878.
8. Klijn, J. G., Berns, P. M., Schmitz, P. I., and Foekens, J. A. (1992) *Endocr. Rev* . **13,** 3-17
9. Sporn, M. B., and Roberts, A. B. (1988) *Nature* **332,** 217-9
10. Mroczkowski, B., Reich, M., Chen, K., Bell, G. I., and Cohen, S. (1989) *Mol. Cell. Biol* . **9,** 2771-8
11. Derynck, R., Roberts, A. B., Winkler, M. E., Chen, E. Y., and Goeddel, D. V. (1984) *Cell* **38,** 287-97
12. Pandiella, A., and Massague, J. (1991) *Proc. Natl. Acad. Sci. USA* **88,** 1726-1730
13. Sporn, M. B., and Roberts, A. B. (1992) *Ann. Intern. Med* . **117,** 408-14
14. Wiley, H. S. (1992) in *Membrane dynamics and signaling* (Bittar, E. E., ed) Vol. 5A, 1 Ed., pp. 113-142, 8 vols., JAI Press, Inc., Greenwich, Conn.
15. Simons, K., and Fuller, D. F. (1985) *Annu. Rev. Cell Biol.* **1,** 243-288
16. Bloom, W., and Fawcett, D. W. (1970) *A textbook of histology*, 9 Ed., W.B. Saunders Co., Philadelphia
17. Koukoulis, G. K., Virtanen, I., Korhonen, M., Laitinen, L., Quaranta, V., and Gould, V. E. (1991) *Am. J. Pathol.* **139,** 787-799
18. Natali, P. G., Nicotra, M. R., Botti, C., Mottolese, M., Bigotti, A., and Segatto, O. (1992) *Br. J. Cancer* . **66,** 318-22
19. Tsutsumi, Y., Naber, S. P., DeLellis, R. A., Wolfe, H. J., Marks, P. J., McKenzie, S.-J., and Yin, S. (1990) *Hum.. Pathol.* **21,** 750-758
20. Parry, G., Beck, J. C., Moss, L., Bartley, J., and Ojakian, G. K. (1990) *Exp. Cell Res* . **188,** 302-11
21. Streuli, C. H., Bailey, N., and Bissell, M. J. (1991) *J. Cell Biol.* **115,** 1383-1395
22. Valverius, E. M., Bates, S. E., Stampfer, M. R., Clark, R., McCormick, F., Salomon, D. S., Lippman, M. E., and Dickson, R. B. (1989) *Mol. Endocrinol.* **3,** 203-14
23. Li, S., Plowman, G. D., Buckley, S. D., and Shipley, G. D. (1992) *J. Cell. Physiol..* **153,** 103-11
24. Snedeker, S. M., Brown, C. F., and DiAugustine, R. P. (1991) *Proc. Natl. Acad. Sci. USA* **88,** 276-280
25. Connolly, J. M., and Rose, D. P. (1988) *Life Sci* . **42,** 1751-1756
26. Johnson, G. R., Saeki, T., Gordon, A. W., Shoyab, M., Salomon, D. S., and Stromberg, K. (1992) *J. Cell Biol.* **118,** 741-51

27. Gabelman, B. M., and Emerman, J. T. (1992) *Exp. Cell Res.* **201,** 113-8
28. Tsutsumi, Y., Naber, S. P., DeLellis, R. A., Wolfe, H. J., Marks, P. J., McKenzie, S. J., and Yin, S. (1991) *Eur. J. Surg. Oncol* . **17,** 9-15
29. Klijn, J. G. M., Berns, P. M. J. J., Bontenbal, M., Alexieva-Figusch, J., and Foekens, J. A. (1992) *J. Steroid Biochem. Mol. Biol.* **43,** 27-43
30. Bates, S. E., Davidson, N. E., Valverius, E. M., Freter, C. E., Dickson, R. B., Tam, J. P., Kudlow, J. E., Lippman, M. E., and Salomon, D. S. (1988) *Mol. Endocrinol* . **2,** 543-55
31. Colomb, E., Berthon, P., Dussert, C., Calvo, F., and Martin, P. M. (1991) *Int. J. Cancer* **49,** 932-937
32. Barrandon, Y., and Green, H. (1987) *Cell* **50,** 1131-1137
33. Blay, J., and Brown, K. D. (1985) *J. Cell. Phys.* **124,** 107-112
34. Mocsatello, D.K., Holgado-Madruga, M., Godwin, A.K., Ramirez, G., Gunn, G., Zoltick, P.W., Biegel, J.A., Hayes, R.L., and Wong, A.J. (1995) *Cancer Res.* **55,** 5536-5539
35. Clarke, R., Brunner, N., Katz, D., Glanz, P., Dickson, R. B., Lippman, M. E., and Kern, F. G. (1989) *Mol. Endocrinol* . **3,** 372-80
36. Nesterov, A., Wiley, H.S., and Gill, G.N. (1995) *Proc. Natl. Acad. Sci. USA* **92,** 8719-8723
37. Moscatello, D.K., Montgomery, R.B., Sundareshan, P., McDanel, H., Wong, M.Y. and Wong, A.J. (1996) *Oncogene* **13,** 85-96
38 Sachs, M., Weidner, K.M., Brinkmann, V., Walther, I., Obermeier, A., Ullrich, A., and Birchmeier, W (1996) *J. Cell Biol.***133,** 1095-1107
39. Stern, D. F., and Kamps, M. P. (1988) *EMBO J.* **7,** 995-1001
40. Kokai, Y., Myers, J. N., Wada, T., Brown, V. I., LeVea, C. M., Davis, J. G., Dobashi, K., and Greene, M. I. (1989) *Cell* **58,** 287-292
41. Holmes, W. E., Sliwkowski, M. X., Akita, R. W., Henzel, W. J., Lee, J., Park, J. W., Yansura, D., Abadi, N., Raab, H., Lewis, G. D., Shepard, H. M., Kuang, W. J., Wood, D. V., Goeddel, D. V., and R.L., V. (1992) *Science* **256,** 1205-1210
42. Culouscou, J. M., Plowman, G. D., Carlton, G. W., Green, J. M., and Shoyab, M. (1993) *J. Biol. Chem.* **268,** 18407-18410
43. Plowman, G. D., Green, J. M., Culouscou, J. M., Carlton, G. W., Rothwell, V. M., and Buckley, S. (1993) *Nature* **366,** 473-475
44. Peles, E., Bacus, S. S., Koski, R. A., Lu, H. S., Wen, D., Ogden, S. G., Levy, R. B., and Yarden, Y. (1992) *Cell* **69,** 205-216
45. Carraway III, K. L., and Cantley, L. C. (1994) *Cell* **78,** 5-8
46. Dougall, W. C., Qian, X., Peterson, N. C., Miller, M. J., Samanta, A., and Greene, M. I. (1994) *Oncogene* **9,** 2109-2123
47. Plowman, G. D., Culouscou, J. M., Whitney, G. S., Green, J. M., Carlton, G. W., Foy, L., Neubauer, M. G., and Shoyab, M. (1993) *Proc. Natl. Acad. Sci. USA* **90,** 1746-1750
48. (4), X. L., Decker, S. J., and Greene, M. I. (1992) *Proc. Natl. Acad. Sci. USA* **89,** 1330-1334
49. Cohen, B. D., Green, J. M., Foy, L., and Fell, H. P. (1996) *J. Biol. Chem.* **271,** 4813-4818
50. Baass, P. C., Di Guglielmo, G. M., Authier, F., Posner, B. I., and Bergeron, J. J. M. (1995) *Trends Cell Biol.* **5,** 465-470

51. Baulida, J., Kraus, M. H., Alimandi, M., Di Fiore, P. P., and Carpenter, G. (1996) *J. Biol. Chem.* **271,** 5251-5257
52. Kornilova, E. S., Taverna, D., Hoeck, W., and Hynes, N. E. (1992) *Oncogene* **7,** 511-519
53. Huang, H. J. S., Nagane, M., Klingbeil, C. K., Lin, H., Nishikawa, R., Ji, X. D., Huang, C. M., Gill, G. N., Wiley, H. S., and Cavenee, W. K. (1997) *J. Biol. Chem.* **272,** 2927-2935
54. Gill, G. N., Kawamoto, T., Cochet, C., Le, A., Sato, J. D., Masui, H., McLeod, C., and Mendelsohn, J. (1984) *J. Biol. Chem.* **259,** 7755-7760
55. Opresko, L. K., and Wiley, H. S. (1990) *J. Cell Biol.* **111,** 1661-1671
56. Kamps, M. P., and Sefton, B. M. (1988) *Oncogene* **2,** 305-315
57. Davies, R. L., Grosse, V. A., Kucherlapati, R., and Bothwell, M. (1980) *Proc. Natl. Acad. Sci. USA.* **77,** 4188-4192
58. Chen, W. S., Lazar, C. S., Lund, K. A., Welsh, J. B., Chang, C. P., Walton, G. M., Der, C. J., Wiley, H. S., Gill, G. N., and Rosenfeld, M. G. (1989) *Cell* **59,** 33-43
59. Stampfer, M. R., Pan, C. H., Hosoda, J., Bartholomew, J., Mendelsohn, J., and Yaswen, P. (1993) *Exp. Cell Res.* **208,** 175-188
60. Band, V., and Sager, R. (1989) *Proc. Natl. Acad. Sci. USA* **86,** 1249-1253
61. Bartek, J., Bartkova, J., Kyprianou, N., Lalani, E. N., Staskova, Z., Shearer, M., Chang, S., and Taylor-Papadimitriou, J. (1991) *Proc. Natl. Acad. Sci. USA* **88,** 3520-3524
62. King, C. R., Borrello, I., Bellot, F., Comoglio, P., and Schlessinger, J. (1988) *EMBO J.* **7,** 1647-1651
63. Opresko, L. K., Chang, C. P., Will, B. H., Burke, P. M., Gill, G. N., and Wiley, H. S. (1995) *J. Biol. Chem.* **270,** 4325-4333
64. Will, B. H., Lauffenburger, D. A., and Wiley, H. S. (1995) *Tissue Eng.* **1,** 81-94
65. Carpenter, G. (1987) *Annu. Rev. Biochem.* **56,** 881-914.
66. Wada, T., Qian, X. L., and Greene, M. I. (1990) *Cell* **61,** 1339-47
67. Stern, D. F., Heffernan, P. A., and Weinberg, R. A. (1986) *Mol. Cell. Biol.* **6,** 1729-1740
68. Spivak-Kroizman, T., Rotin, D., Pinchasi, D., Ullrich, A., Schlessinger, J., and Lax, I. (1992) *J. Biol. Chem.* **267,** 8056-8063
69. Qian, X., LeVea, C. M., Freeman, J. K., Dougall, W. C., and Greene, M. I. (1994) *Proc. Natl. Acad. Sci. USA* **91,** 1500-1504
70. Wright, J. D., Reuter, C. W. M., and Weber, M. J. (1995) *J. Biol. Chem.* **270,** 12085-12093
71. Guy, P. M., Platko, J. V., Cantley, L. C., Cerione, R. A., and Carraway 3rd, K. L. (1994) *Proc. Natl. Acad. Sci. USA* **91,** 8132-8136
72. Kurten, R. C., Cadena, D. L., and Gill, G. N. (1996) *Science* **272,** 1008-1010
73. French, A. R., Sudlow, G. P., Wiley, H. S., and Lauffenburger, D. A. (1994) *J. Biol. Chem.* **269,** 15749-15755
74. Herbst, J. J., Opresko, L. K., Walsh, B. J., Lauffenburger, D. A., and Wiley, H. S. (1994) *J. Biol. Chem.* **269,** 12865-12873
75. Klijn, J. G., Berns, P. M., Schmitz, P. I., and Foekens, J. A. (1992) *Endocrin. Rev.* **13,** 3-17
76. Di Fiore, P. P., Pierce, J. H., Kraus, M. H., Segatto, O., King, C. R., and Aaronson, S. A. (1987) *Science* **237,** 178-182

77. Kraus, M. H., Popescu, N. C., Amsbaugh, S. C., and King, C. R. (1987) *EMBO J.* **6,** 605-610
78. Marth, C., Marcus, T. L., Cronauer, M. V., Doppler, W., Zeimet, A. G., Bachmair, F., Ullrich, A., and Daxenbichler, G. (1992) *Int. J. Cancer* **52,** 311-316
79. Wells, A., Welsh, J. B., Lazar, C. S., Wiley, H. S., Gill, G. N., and Rosenfeld, M. G. (1990) *Science* **247,** 962-964

Figure Legends

Figure 1. Matrigel induces HMEC to form gland-like structures in vitro. Cells were plated in medium MCDB 170 on either plastic for 3 days (top panel) or Matrigel for 11 days (bottom panel). The medium was changed every 3 days. Cells grown on Matrigel form both tubular and alveolar structures which resemble their in vivo counterparts.

Figure 2. Histology of alveolar structures formed by HMEC on Matrigel. Cells grown for 3 weeks as described in the legend of Fig. 1 were fixed and stained for histology. Cells did not form empty lumens, but instead underwent squamous differentiation. Blue arrow indicates a keratin pearl indicative of squamous differentiation.

Figure 3. Time-lapse sequence of HMEC forming organized structures. Sequence starts 12 h after plating on Matrigel. Photos were taken at 25X approximately 3-5 h apart. Arrows indicate clumps of cells being consolidated into larger structures.

Figure 4. Final stages of consolidation of HMEC into organized structures. Sequence starts approximately 38 h following plating of cells on Matrigel. Photos were taking at 25X approximately 8 h apart. Arrows point to the same clump of cells in each photo.

Figure 5. Blocking the EGFR inhibits organization of HMEC on Matrigel. Photos were taken of cells grown on Matrigel in the presence of 12.5 ng/ml EGF for the indicated time periods. Cells in the bottom-right panel were incubated in 10μg/ml 225 mAb for 10 days.

Figure 6. Effect of EGF and 225 mAb on spreading of HMEC on Matrigel. Plates were coated with a thin layer of Matrigel, after which cells were plated in the absence (left) or presence (middle) of 12ng/ml EGF. Alternately, cells were incubated with 10μg/ml 225 mAb. Photos were taken at 200X approximately 18 h following plating.

Figure 7. Screening cells for expression of the Δ2-7 EGFR. Cells were transduced with a retrovirus containing the Δ2-7 EGFR gene and sorted by flow cytometry for expression of Δ2-7 EGFR using a specific antibody. Individual clones were isolated, extracted and the proteins were separated by electrophoresis. Shown is a western blot using the pan-EGFR antibody N13. The WT lane is an extract for B82 cells expressing full-length EGFR. The Δ2-7 lane contains an extract of U87 cells expressing almost exclusively the 2-7 EGFR. The numbers over each lane are the designations of individual clones.

Figure 8. Confluent cultures of the indicated cells were split 1:800 into 60 mm dishes and allowing them to grow for three weeks in the presence of control medium, or with either 10 μg/ml monoclonal antibody 225 or 12.5 ng/ml EGF. The cells were then stained with crystal violet. ΔEGFR 16 and ΔEGFR 11 refer to the clones shown in Fig. 7.

Figure 9. Growth Curve of HMEC +/- EGF. Cells expressing no (parental), low levels (clone 16) or high levels (clone 11) of Δ2-7 EGFR were incubated in medium containing 12.5 ng/ml EGF (left panel) or 10 μg/ml 225 monoclonal anti-EGFR antibody (right

panel). At 24 h intervals, cells were removed from the culture dish and counted on a Coulter counter.

Figure 10. Antagonistic antibody 225 does not block the activity of Δ2-7 EGFR. Parent (WT) or clone 11 cells were grown in the absence or presence of 12.5 ng/ml EGF for 10 min or 10μg/ml 225 mAb for 24 h. Cells were extracted and then the WT and Δ2-7 EGFR were sequentially immunoprecipitated and analyzed by western blot. Top panel is probed with an anti-phosphotyrosine antibody whereas the bottom panel is probed with a pan-EGFR antibody to the amino-terminus 13 amino acids of the EGFR. Note that the low molecular weight EGFR band in the left panel is not detected by the pan-EGFR antibody. Because this antibody and the Δ2-7 EGFR-specific antibody recognize overlapping sequences, this suggests that this form of the receptor lack the overlapping fragment at the amino-terminus.

Figure 11. Expression of Δ2-7 EGFR inhibits cell migration in HMEC. Cells were brought to quiescence in 60 mm plates prior to scraping a single, central area with a rubber policeman. The wound was measured via ocular micrometer, the area under observation marked and the cells incubated in medium containing no EGF or 12.5 ng/ml EGF. At daily intervals the wound was measured and the change in wound size recorded. The ΔEGFR cells were clones 3, 16 and 11.

Figure 13 on page 19

Figure 12. The Δ2-7 EGFR is constitutively associated with SHC in HMEC. Parental HMEC (WT) or cells expressing sEGF (A1E) or Δ2-7 EGFR at a low (clone 16) or high levels (clone 11) were treated without (left panel) or with (right panel) 12.5 ng/ml of EGF for 15 min at 37°C. The cells were solubilized and SHC was immunoprecipitated and separated by gel electrophoresis. Top panel is a western blot probed with an anti-PY antibody. Bottom panel is total lysate probed with an anti-SHC antibody.

Figure 14. Relative secretion rates of EGF by HMEC transfected with gene for a secreted form of EGF (sEGF) or a membrane-bound form (EGF-Ct). Cells were plated in the presence or absence of 10μg/ml 225 mAb. Samples of medium were collected at 24 and 48 h, evaluated for EGF levels by ELISA and cell number was determined. Values are the change in amount of EGF in the medium corrected for the average number of cells during the sampling interval.

Figure 15. Distribution of EGFR and EGF in cells expressing a secreted form of EGF (sEGF) or a membrane-bound form (EGF-Ct). Cells plated on fibronectin-coated cover slips 24 h previously were fixed and permeabilized with saponin. They were then stained with a mouse mAb against the EGFR (left panels) and a rabbit polyclonal against EGF. Images were then collected at two separate wavelengths. All exposures were for the same time for each wavelength.

Figure 16. Co-localization of EGF and the EGFR in the same vesicles. The middle panels shown in Fig. 15 were normalized to a full dynamic range to show the relative distribution of the EGFR (left panel) and EGF (right panel).

Figure 17. Cells expressing a secreted form of EGF have a non-interruptible autocrine loop. Confluent cultures of the indicated cells were split 1:800 into 60 mm dishes and allowing them to grow for three weeks in the presence of control medium, or with either 10 μg/ml monoclonal antibody 225 or 12.5 ng/ml EGF. The cells were then stained with crystal violet.

Figure 18. Antagonistic antibodies to the EGFR cannot block signaling in cells expressing a secreted form of EGF. Panel A: Cells expressing the indicated EGF construct were plated out at a 1:10 dilution and grown in the absence (−○−) or presence (−●−) of EGF. Alternately, they were grown in the presence of 10μg/ml of 225 mAb (−△−). Cell number was determined at the indicated times. Panel B: confluent cultures of cells expressing the indicated EGF construct were incubated with 12.5 μg/ml of EGF for 15 min or with 10 μg/ml of 225 mAb 18 h. The were then extracted in detergent, SHC was immunoprecipated and subjected to western blot analysis using anti-PY as a probe.

Figure 19. Cells expressing a secreted form of EGF cannot form organotypic structures on Matrigel. The indicated cells were plated at 50,000 cells per well on thin layers of Matrigel in the presence or absence of EGF. Alternately, 225 mAb was added. Shown are representative micrographs of the cell layers 5 days after plating.

Figure 20. Effect of EGF on erbB-2 and EGF-R levels in human mammary epithelial cells as evaluated by flow cytometry. HMEC 184A1L5 cells were grown for 48 h in the absence of EGF and treated for 1 h at 37°C either without (shaded peaks) or with (light peaks) 100 ng/ml of EGF. Cells were then removed from their plates, fixed and stained with either anti-EGF-R mAb 225 (top panel) or anti-erbB-2 mAb Ab5 (lower panel) as described in Materials and Methods. Secondary antibody alone (FITC-labeled goat anti-mouse) is shown in the top panel (white peak). Data represents FACS results of approximately 5200 cells/profile.

Figure 21. Kinetics of EGF-mediated down regulation of EGF-R and erbB-2 in human mammary epithelial cells and mouse fibroblasts. Cells were treated for the indicated times with 100 ng/ml of EGF, removed from their plates by scraping and extracted with detergent. EGF-R levels (−●−) were determined using a specific ELISA and erbB-2 levels (−□−) were determined using storage phosphor plates following western blot analysis as described in Material and Methods. Top panel is an image of western blots of erbB-2 at the indicated time after EGF treatment. Data is the average of from 4 to 8 experiments +/- SEM.

Figure 22. Levels of erbB-2 mRNA do not change after EGF treatment. Monolayers of either 184A1L5 HMEC (left) or B82 mouse fibroblast expressing human EGF-R (right) were treated without or with 100 ng/ml of EGF for 4 h at 37°C. Total RNA was extracted, reverse transcribed and specific erbB-2 transcripts (top panel) and control G3PDH were amplified by PCR as described in Materials and Methods using the indicated amounts of cDNA. Shown is a scanned image of the reaction products run of 1.8% agarose gels and stained with ethidium bromide.

Figure 23. Distribution of EGF-R and erbB-2 in mouse B82 fibroblasts. Cells were fixed and permeabilized and the distributions of EGF-R (left panels) and erbB-2 (right panels) were determined by use of mouse monoclonal antibody 528 and rabbit polyclonal antibody C18 respectively. Panels A and B are untreated cells, panels B and C are also untreated cells, but incubation with primary antibodies was done in the presence of competing erbB-2 peptide C18. Panels E and F are cells following treatment for 4 h at 37°C with 100 ng/ml of EGF. Arrows indicate identical vesicles. Images were acquired with a Photometrics cooled CCD camera as described in Materials and Methods. Exposures times and scaling of all images were identical for each receptor type.

Figure 24. Distribution of EGF-R and erbB-2 in different cell types as determined by confocal microscopy. Cells grown on cover slips were fixed, permeabilized and simultaneously stained for EGF-R (left panels) and erbB-2 (right panels) using monoclonal and polyclonal antibodies respectively. Optical sections 0.5 microns thick were taken through the lower 1/3 of the cells. The two images were collected separately using barrier filters to prevent spillover between the FITC images (left) and Texas Red images (right). Top panels are mouse B82 fibroblasts. Middle panels are human HB2 mammary epithelial cells and bottom panels are human breast carcinoma line SKBR3.

Figure 25. Kinetics of EGF-induced downregulation of erbB-2 in cells expressing different mutants of the EGF-R. Mouse B82 cells expressing either kinase-active (panel A) or kinase-inactive (panel B) EGF-R were incubated with 100 ng/ml of EGF for the indicatedlengths of time. The cells were extracted with detergent and the remaining erbB-2 mass was determined by quantitative western blot analysis using a Bio-Rad Molecular Imager. The EGF-R types used were wild type (−●−, n= 7), kinase inactive M^{721} (−■−, n=5), c'958 (−○−, n=4), c'958 M^{721} (−□−, n=3), c'688 (—△—, n=2) and c'647 (—▽—, n=3). The error bars represent the SEM of the indicated number of independent experiments.

Figure 26 Effect of EGF on tyrosine phosphorylation of erbB-2. Mouse fibroblasts expressing the indicated EGF-R mutants were treated either without (open bars) or with 100 ng/ml of EGF for 15 or 120 minutes (shaded bars) and then extracted with detergent. The erbB-2 was immunoprecipitated from equal amounts of cell extract (corrected for protein) and the samples were split and run on two separate gels. Following transfer to nitrocellulose, they were probed for phosphotyrosine (top panel) or erbB-2 protein (middle panel). The images were acquired using a Bio-Rad Molecular Imager. Bottom panel is the ratio of phosphotyrosine to erbB-2 of the western blots as determined using the Molecular Analyst software package.

Figure 27. Removal of the kinase domain of the EGF-R eliminates EGF-induced tyrosine phosphorylation of erbB-2. Mouse fibroblasts expressing the indicated EGF-R mutants were treated either without (open bars) or with (shaded bars) 100 ng/ml of EGF for 15 min, Following immunoprecipation of erbB-2, the levels of phosphotyrosine (top panel), erbB-2 (middle panel) and the PY:erbB-2 ratios (bottom panels were determined as described in the legend of Fig. 7.

Figure 28. The ability of EGF to induce down regulation of erbB-2 levels is correlated with tyrosine phosphorylation of erbB-2. Mouse fibroblasts expressing the indicated EGF-R mutants were treated with 100 ng/ml of EGF for 6-8 h at 37C. The cells were extracted and the total levels of erbB-2 remaining was determined by quantitative western blots (top panel). The fold increase in phosphotyrosine levels in erbB-2 following 15 min EGF treatment (bottom panel) was determined following immunoprecipitation of erbB-2 in parallel samples as described in the legend of Fig. 7.

Figure 1

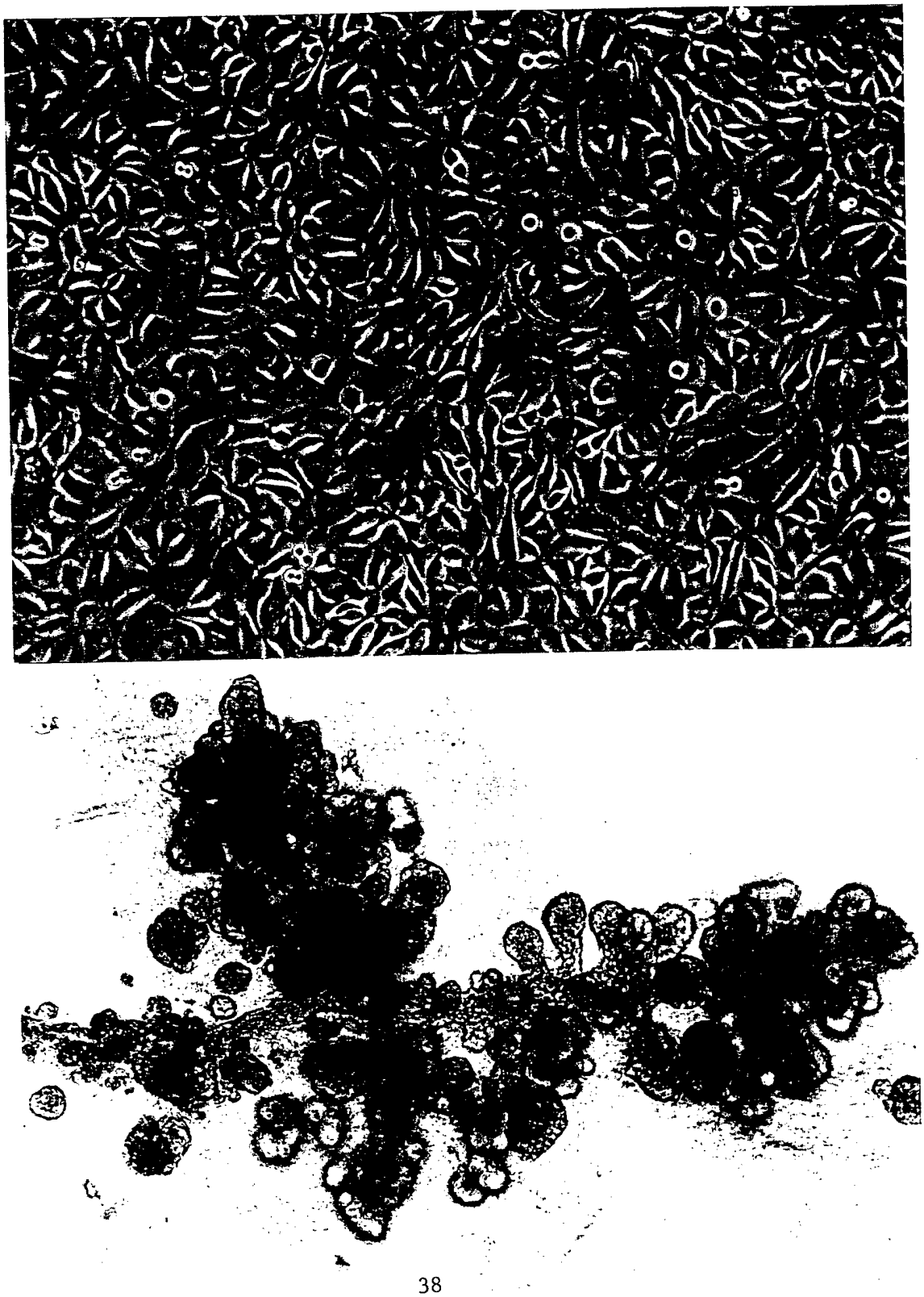

Figure 2

Figure 2

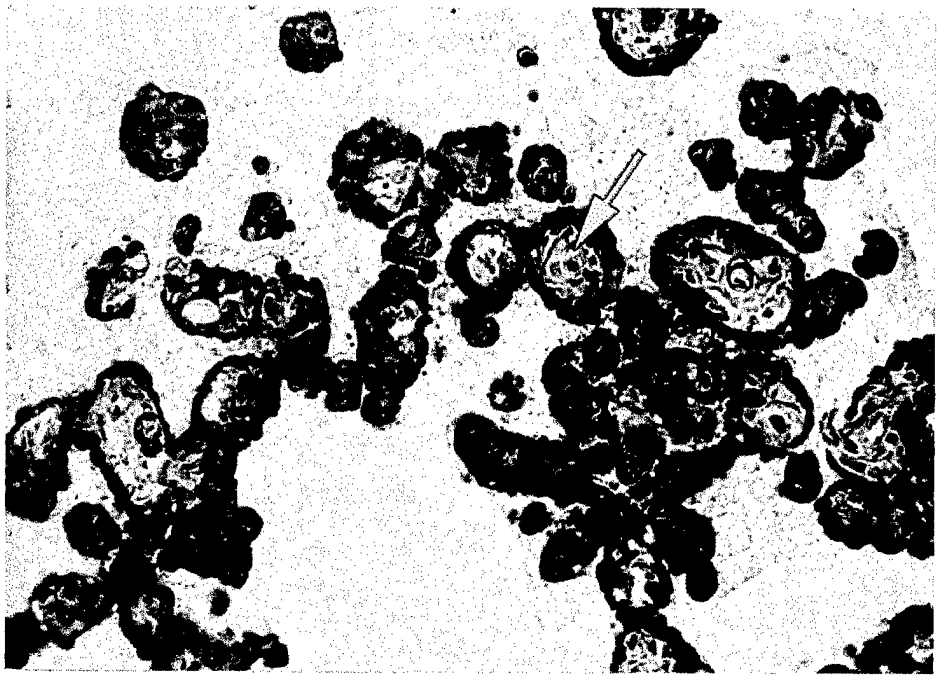

Figure 3

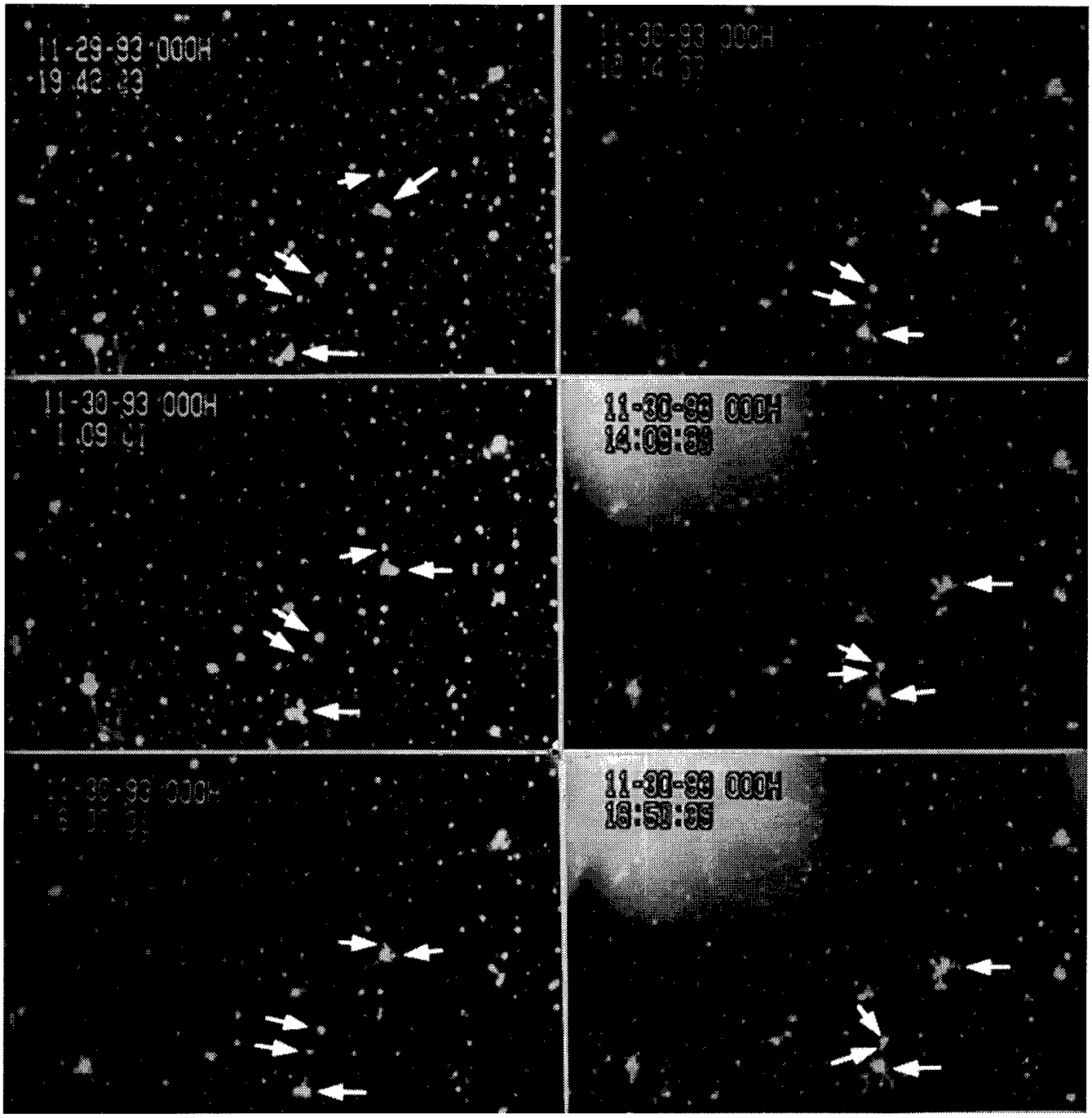

Figure 4

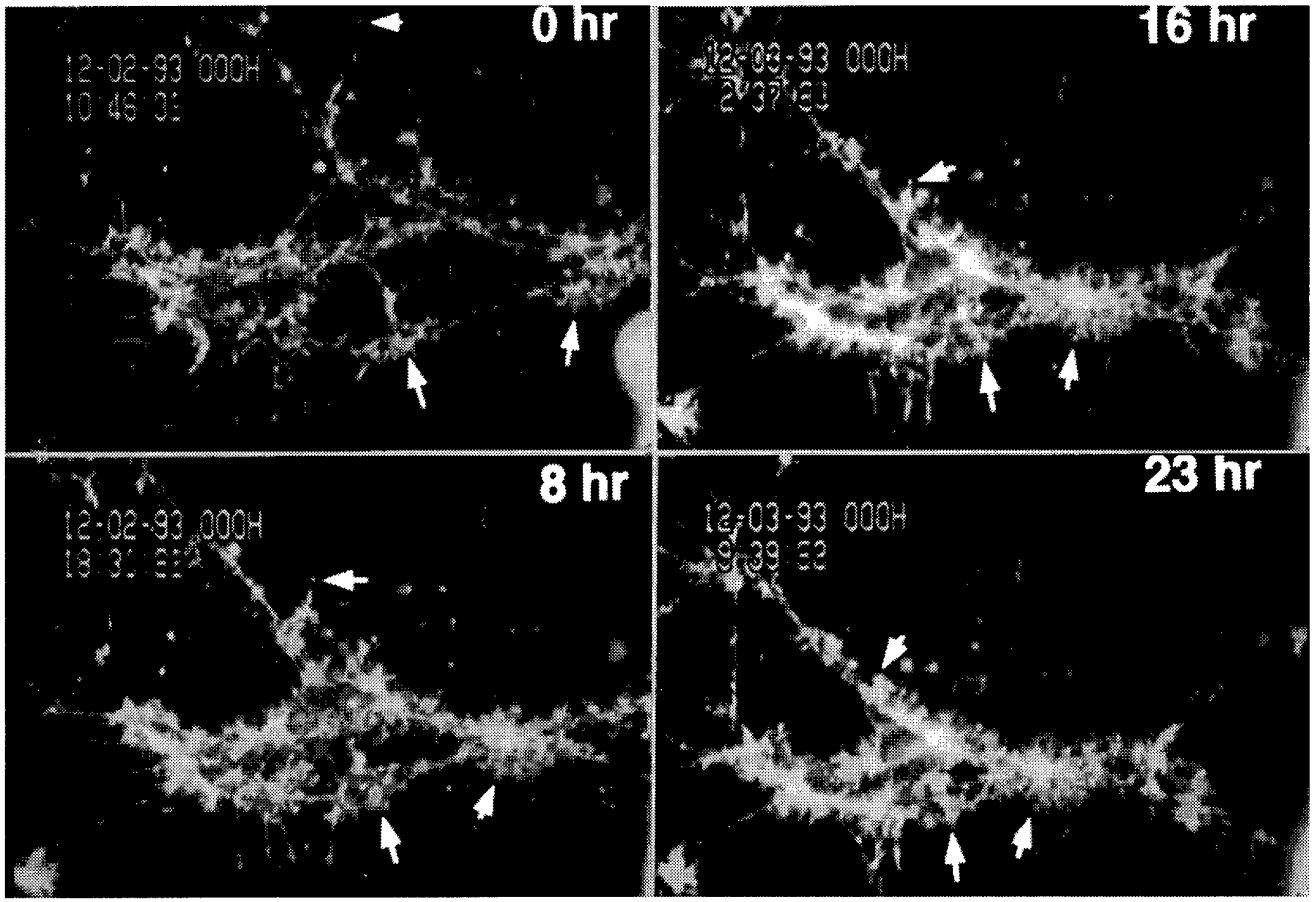

Figure 5

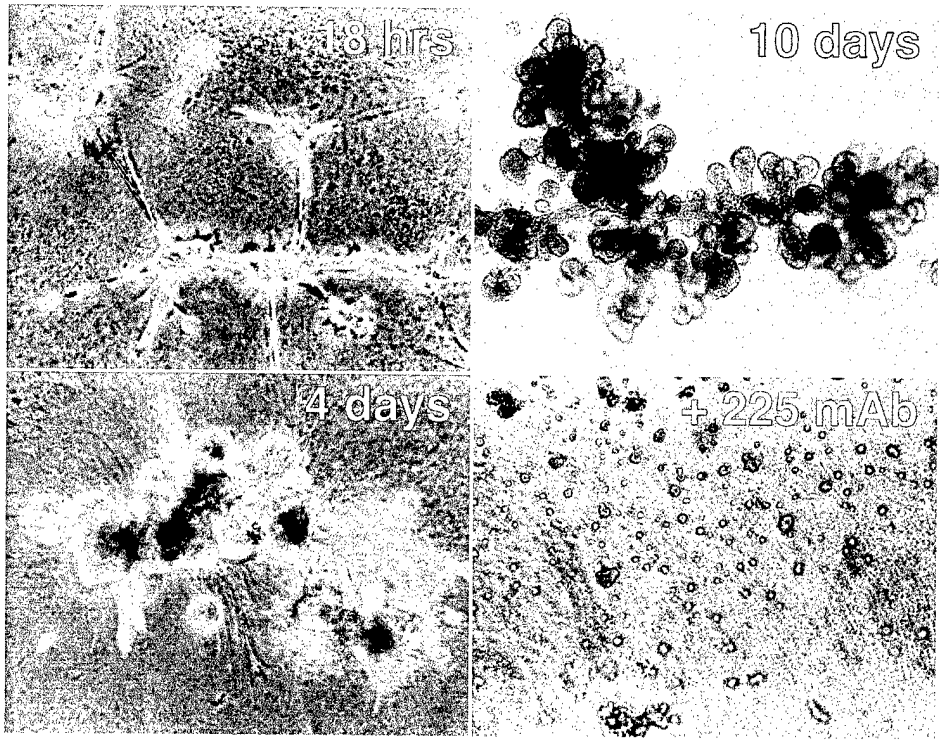

Figure 6

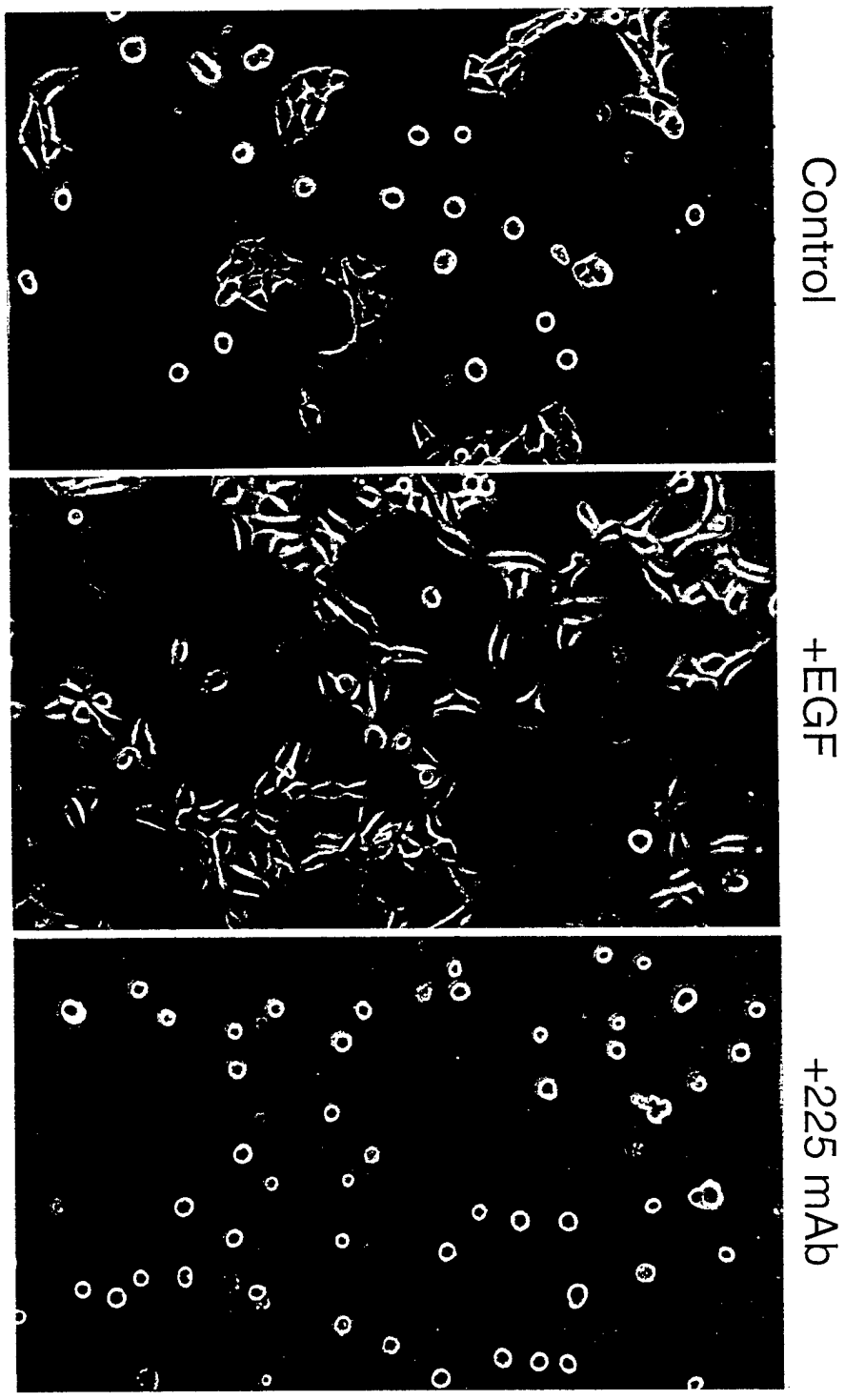

Figure 7

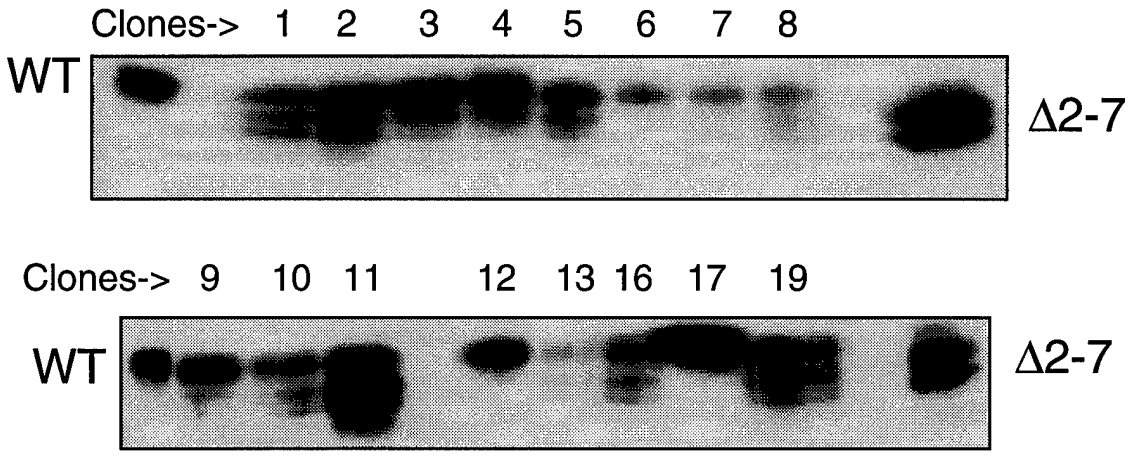

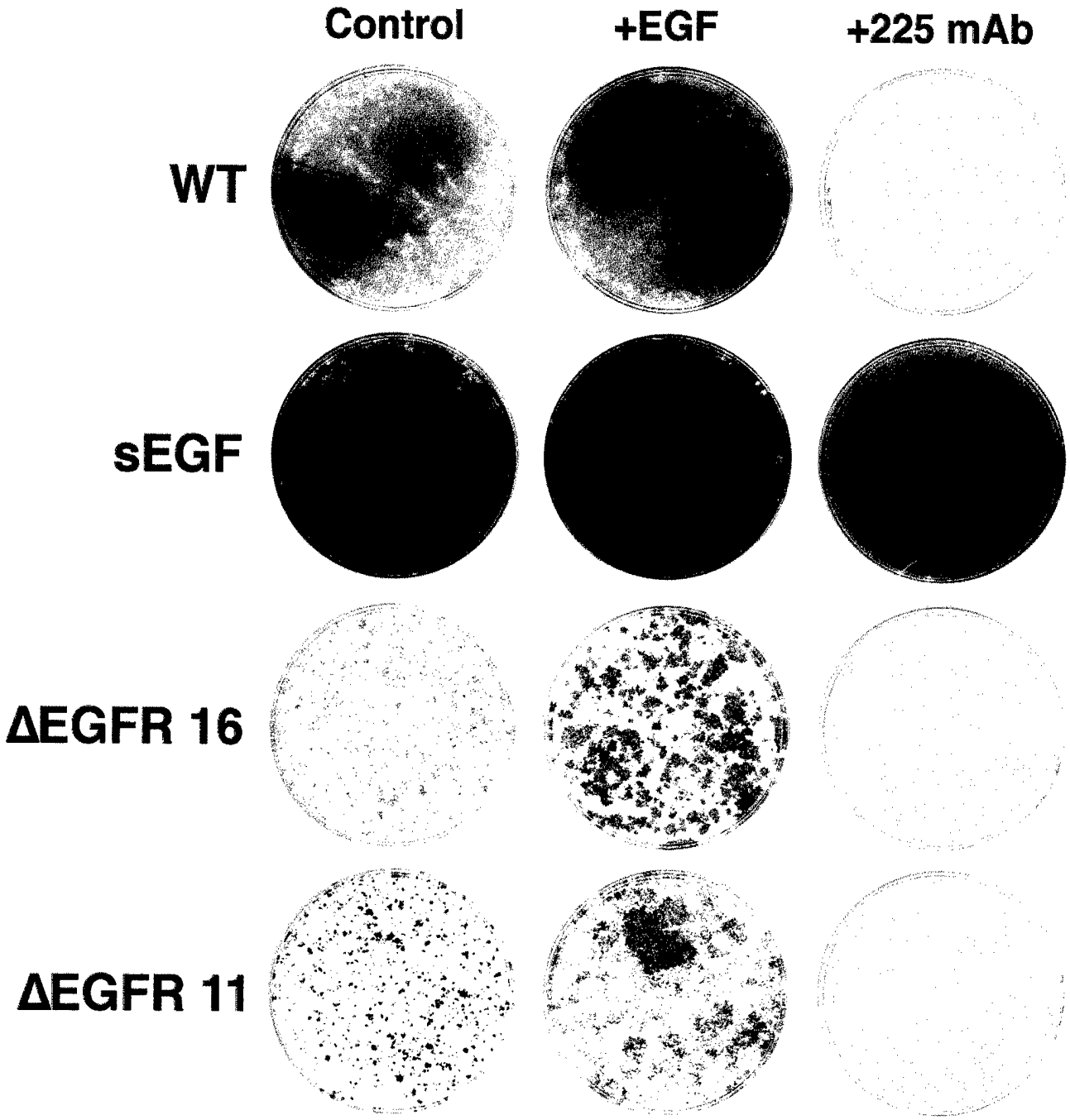
Control
+EGF
+225 mAb
WT
sEGF
ΔEGFR 16
ΔEGFR 11

Figure 9

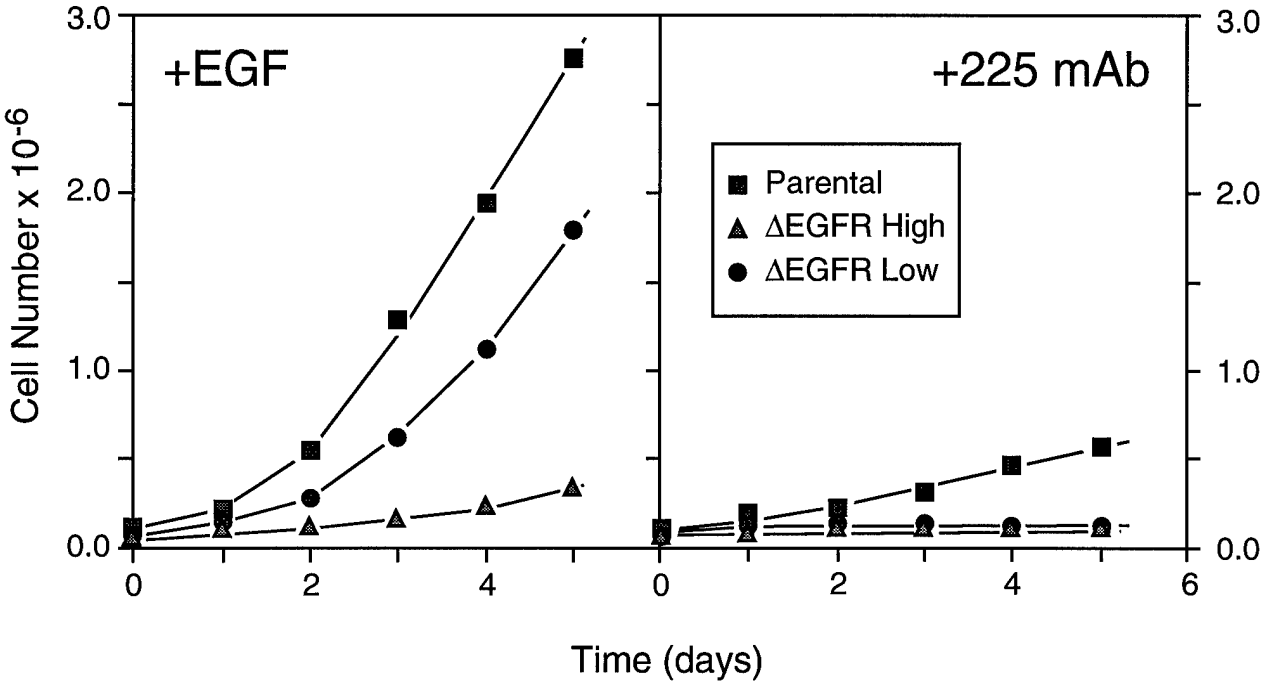
+EGF
+225 mAb
Parental
ΔEGFR High
ΔEGFR Low
Cell Number x 10-6
Time (days)
3.0
2.0
1.0
0.0
0
2
4
6

Figure 10

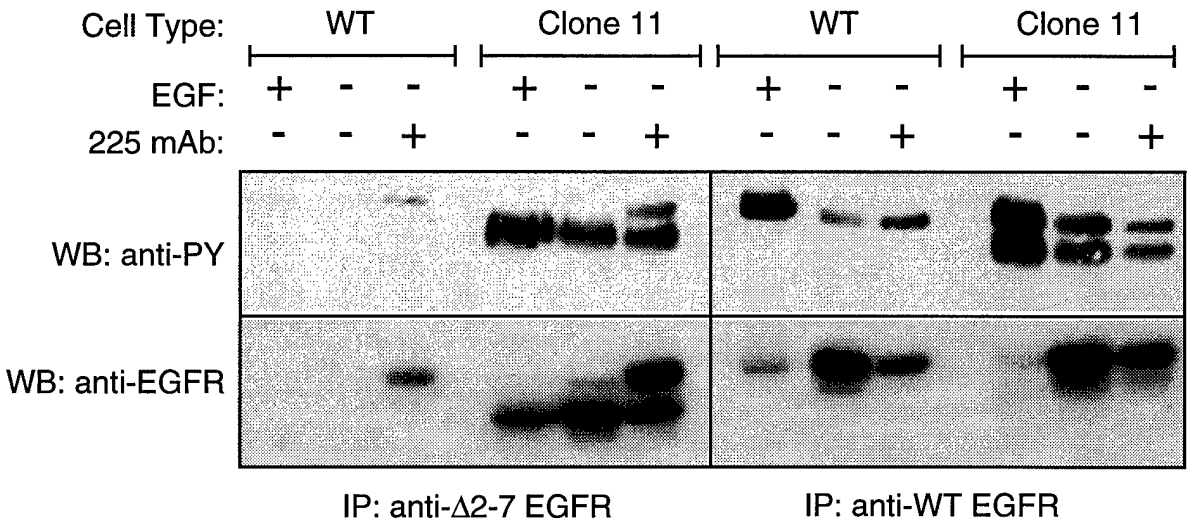
Cell Type:
WT
Clone 11
WT
Clone 11
EGF:
225 mAb:
WB: anti-PY
WB: anti-EGFR
IP: anti-Δ2-7 EGFR
IP: anti-WT EGFR

Figure 11

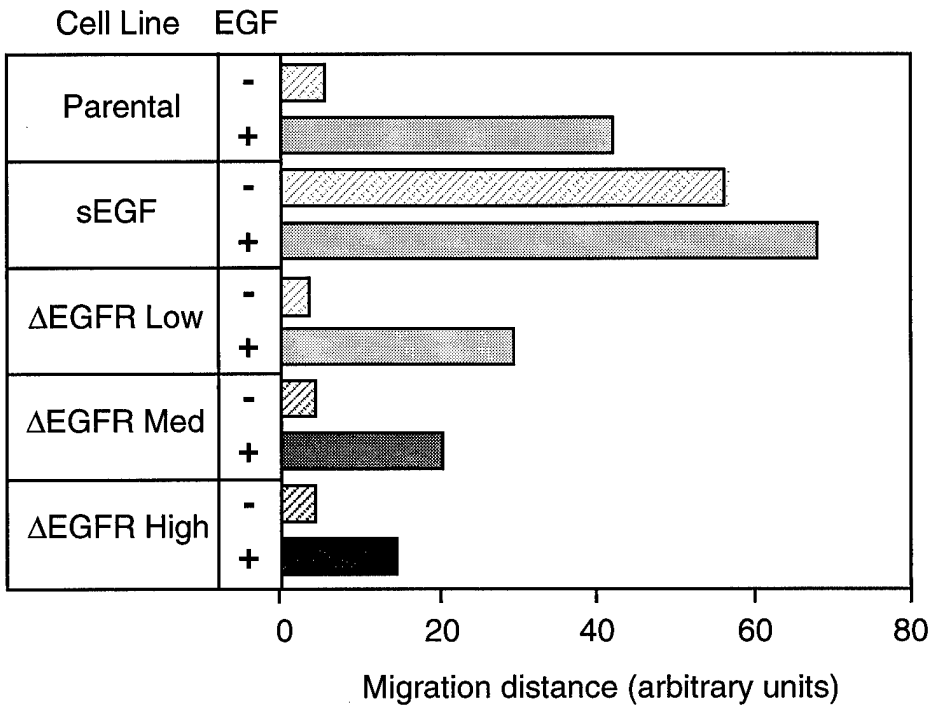
Cell Line
EGF
Parental
sEGF
ΔEGFR Low
ΔEGFR Med
ΔEGFR High
-
+
0
20
40
60
80
Migration distance (arbitrary units)

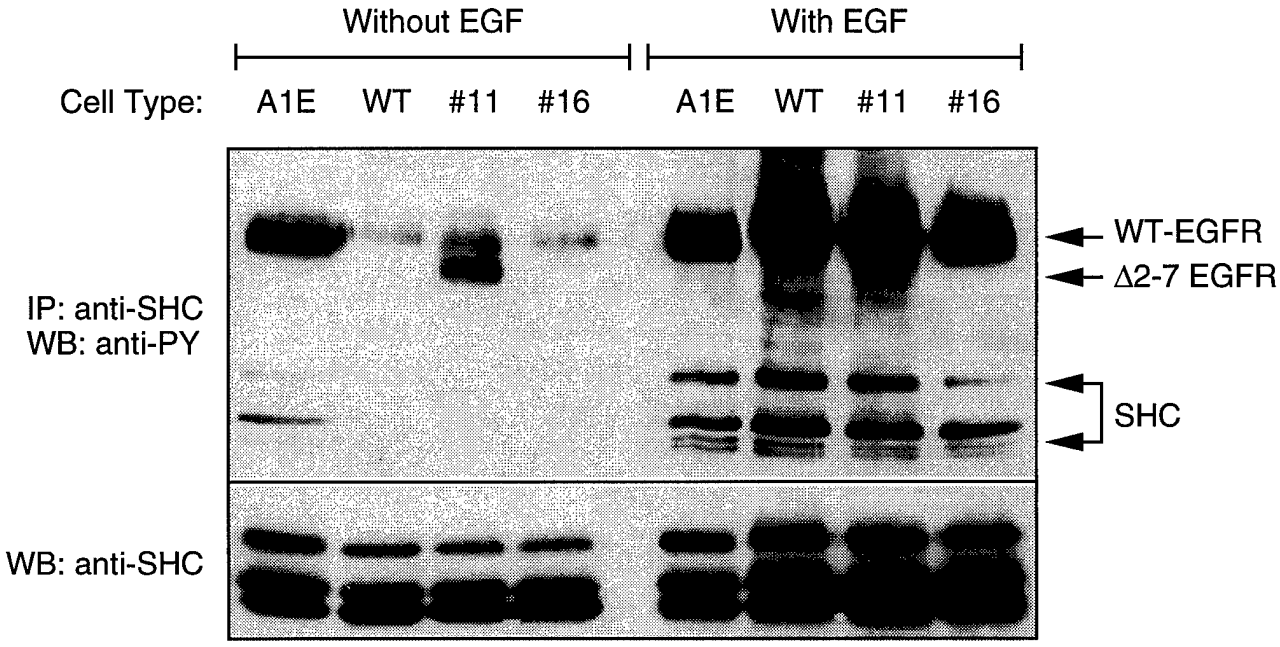
Without EGF
With EGF
Cell Type:
A1E
WT
#11
#16
A1E
WT
#11
#16
IP: anti-SHC
WB: anti-PY
WB: anti-SHC
WT-EGFR
Δ2-7 EGFR
SHC

Figure 14

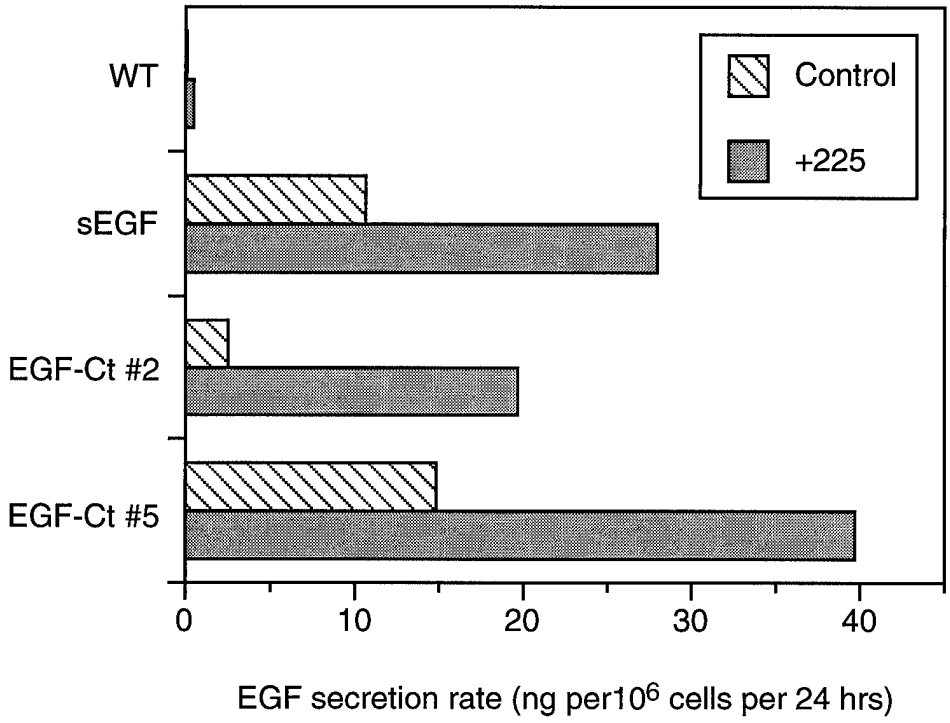
WT
sEGF
EGF-Ct #2
EGF-Ct #5
Control
+225
0
10
20
30
40
EGF secretion rate (ng per10^6 cells per 24 hrs)

Figure 15

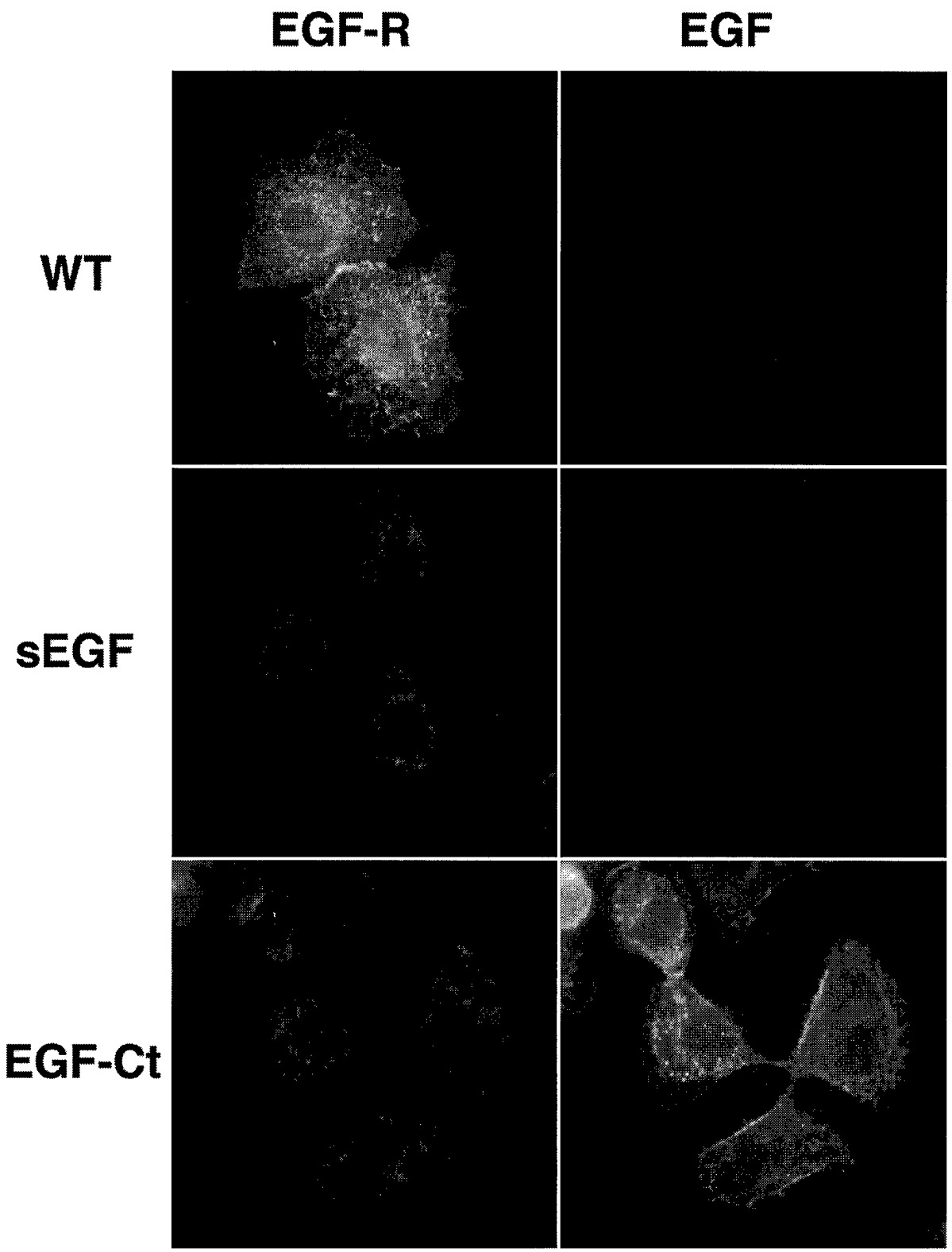

Figure 16

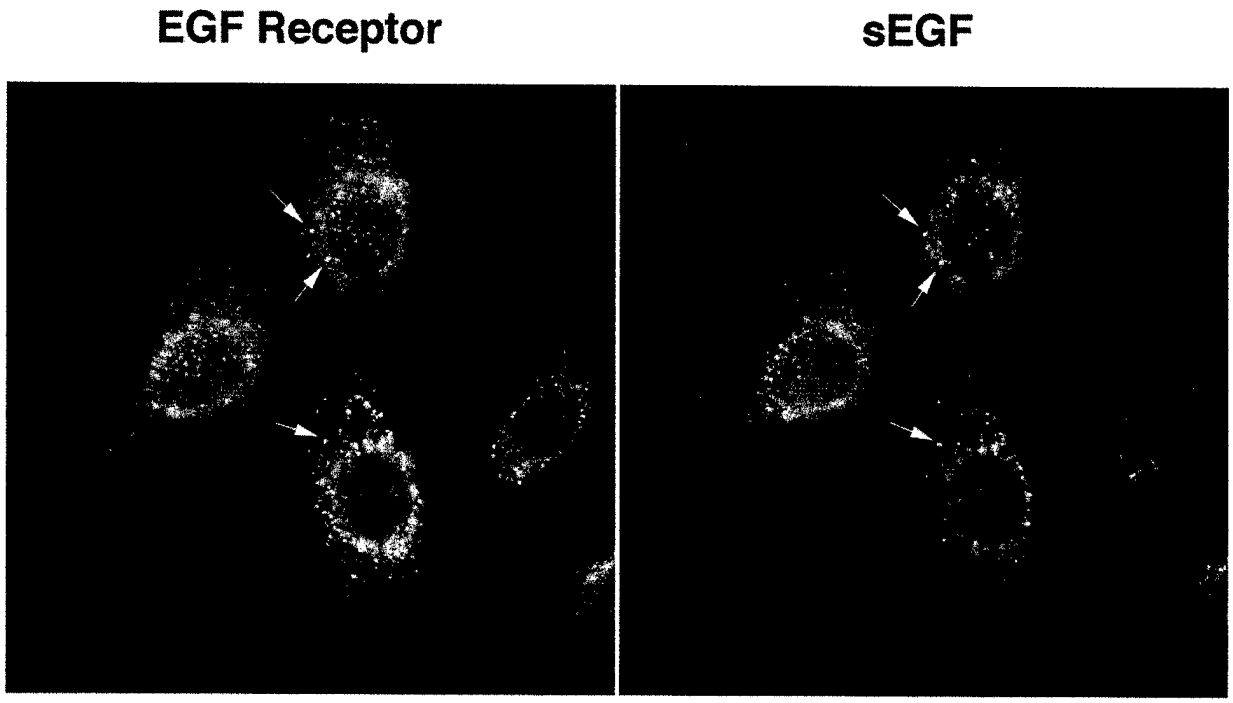

Figure 17

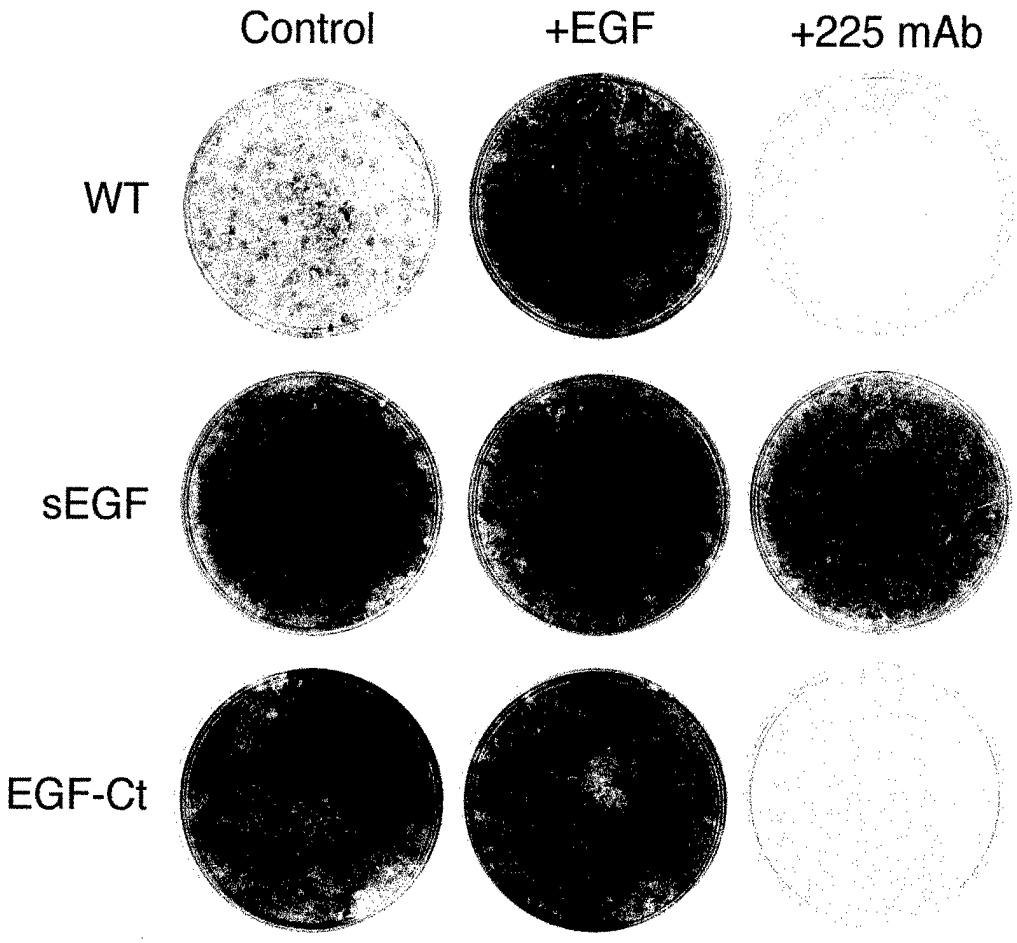

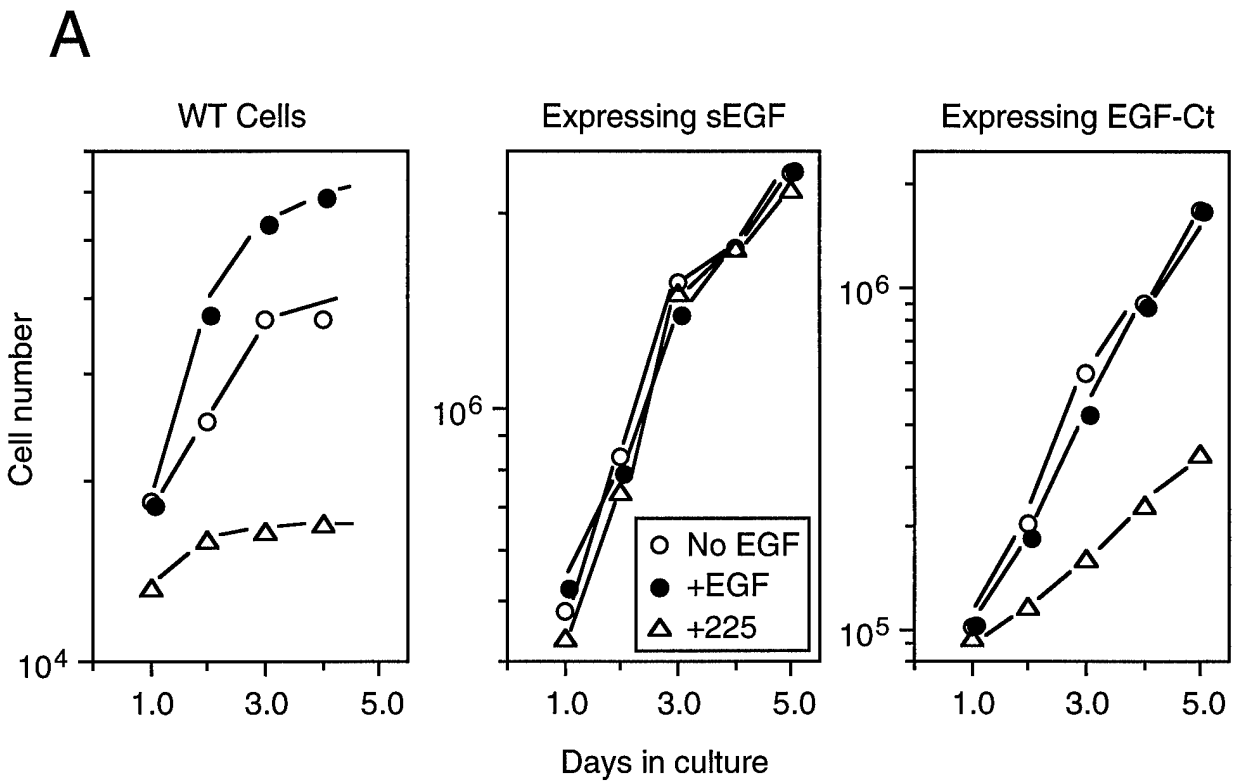
A
WT Cells
Expressing sEGF
Expressing EGF-Ct
Cell number
10^4
10^6
10^6
10^5
1.0
3.0
5.0
No EGF
+EGF
+225
Days in culture

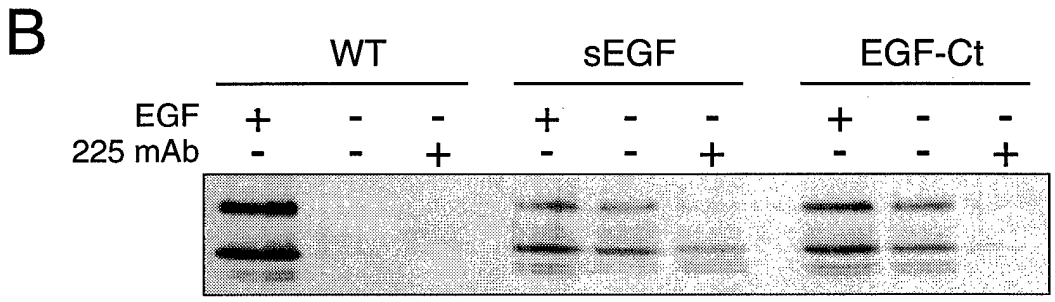
B
WT
sEGF
EGF-Ct
EGF + - - + - - + - -
225 mAb - - + - - + - - +

Figure 19

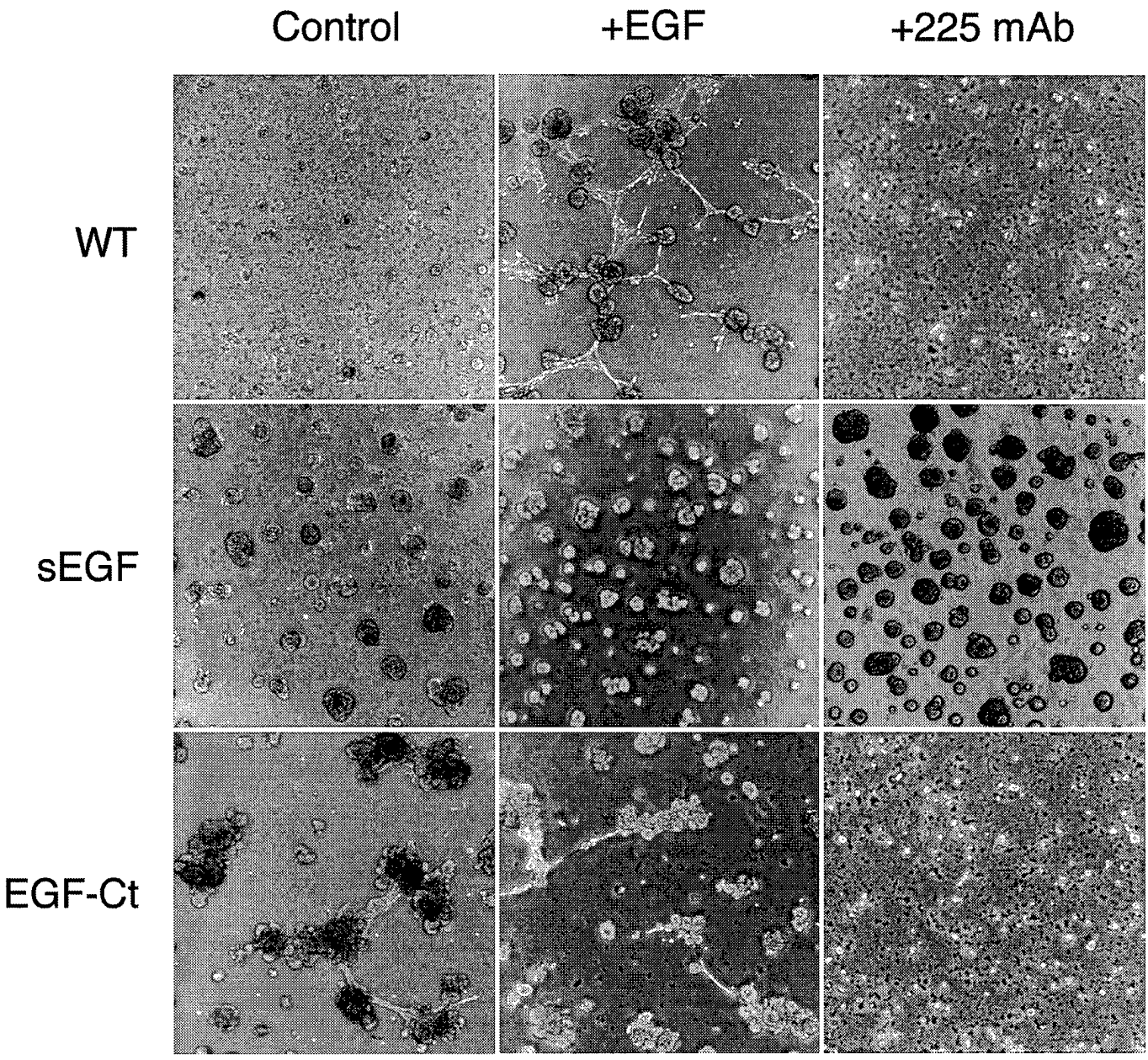

Figure 20

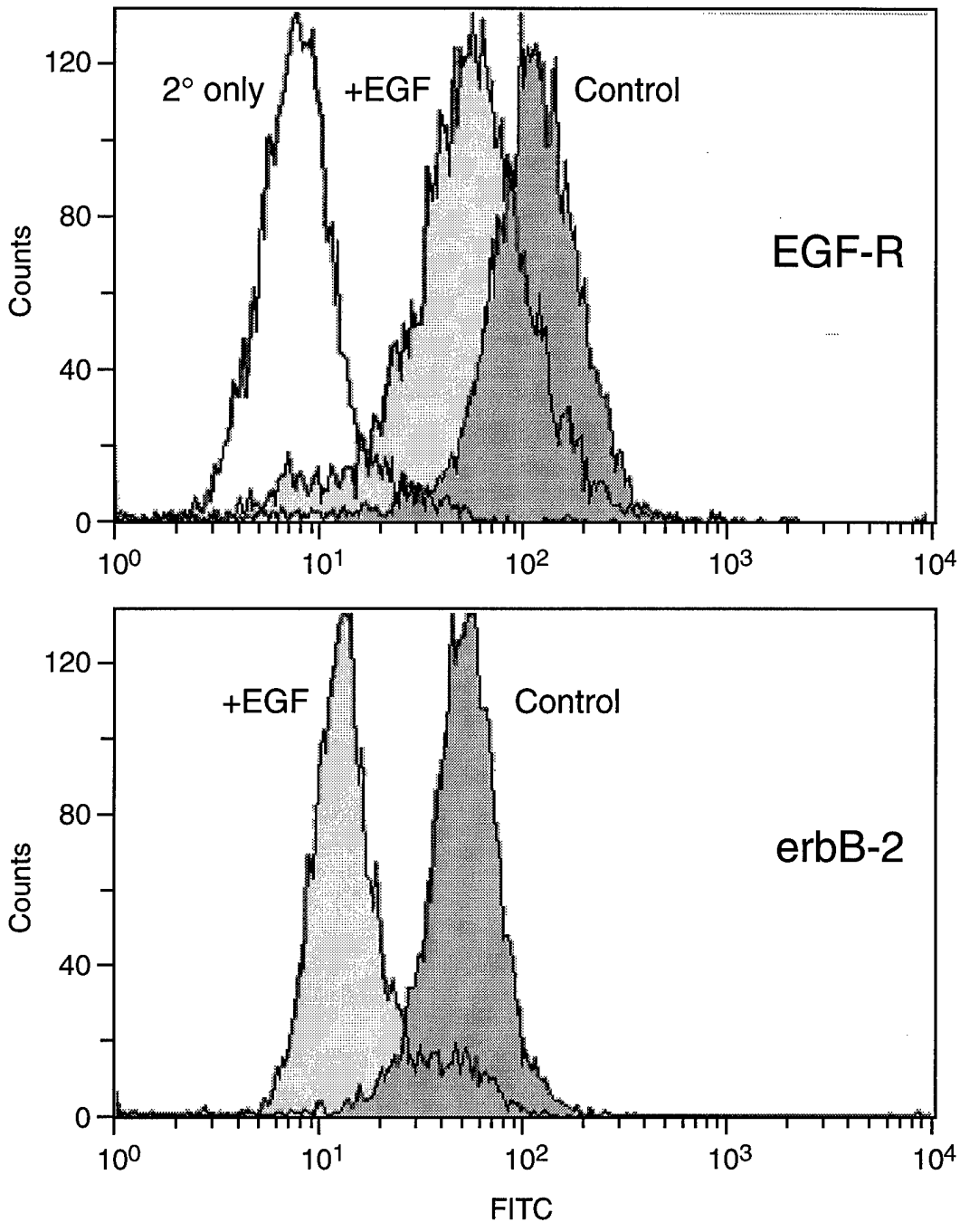
2° only
+EGF
Control
EGF-R
Counts
120
80
40
0
10^0
10^1
10^2
10^3
10^4
+EGF
Control
erbB-2
Counts
120
80
40
0
10^0
10^1
10^2
10^3
10^4
FITC

Figure 21

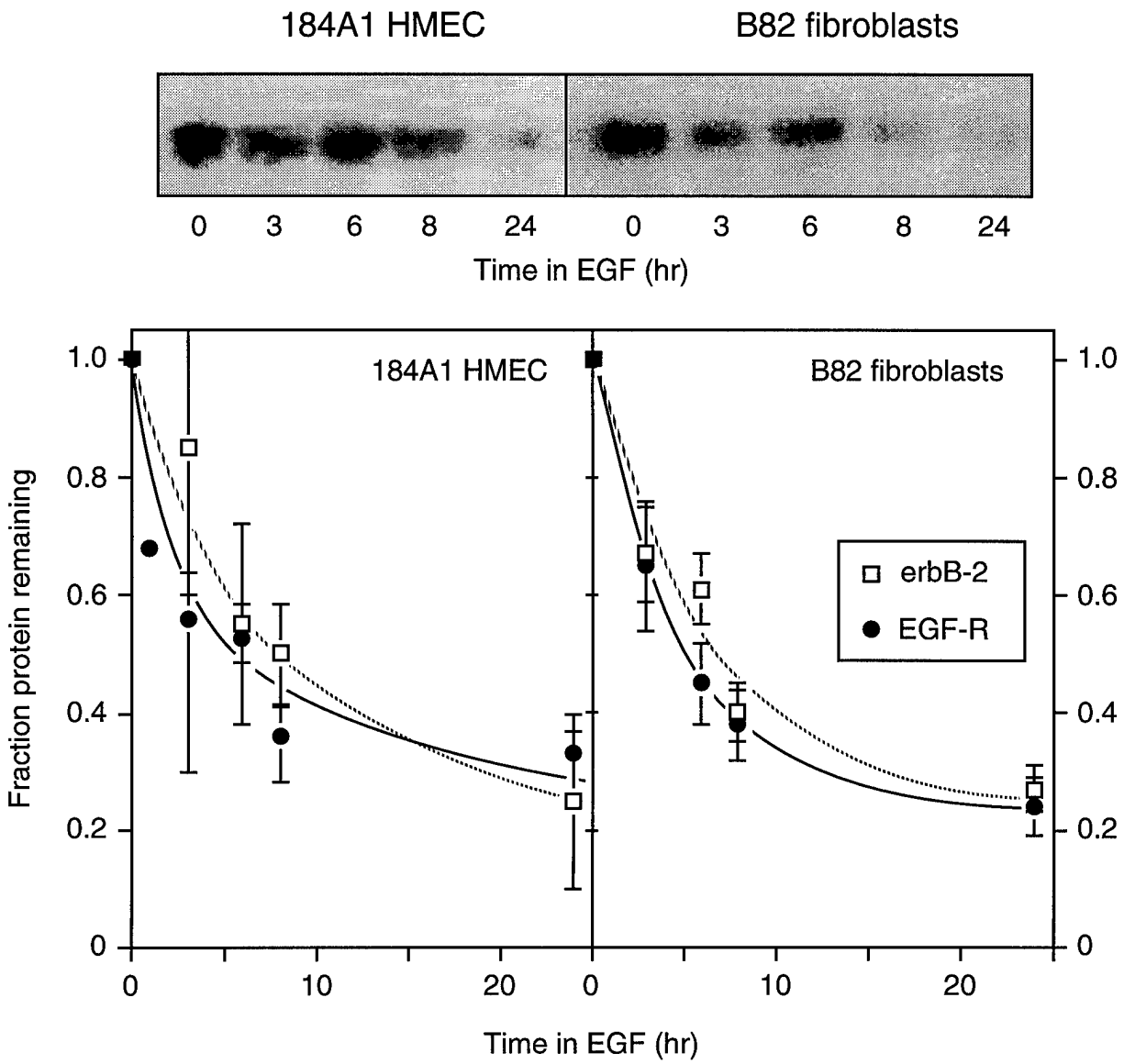
184A1 HMEC
B82 fibroblasts
0 3 6 8 24 0 3 6 8 24
Time in EGF (hr)
184A1 HMEC
B82 fibroblasts
erbB-2
EGF-R
Fraction protein remaining
1.0
0.8
0.6
0.4
0.2
0
0 10 20 0 10 20
Time in EGF (hr)

Figure 22

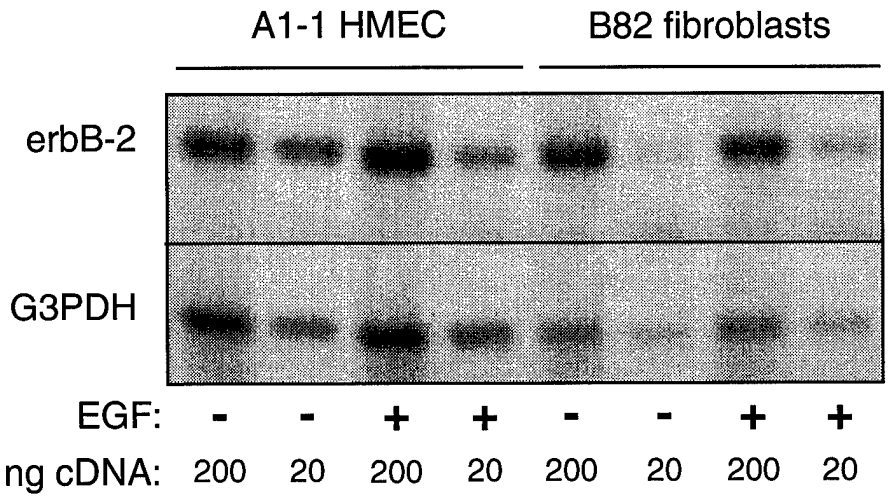
A1-1 HMEC
B82 fibroblasts
erbB-2
G3PDH
EGF: - - + + - - + +
ng cDNA: 200 20 200 20 200 20 200 20

Figure 23

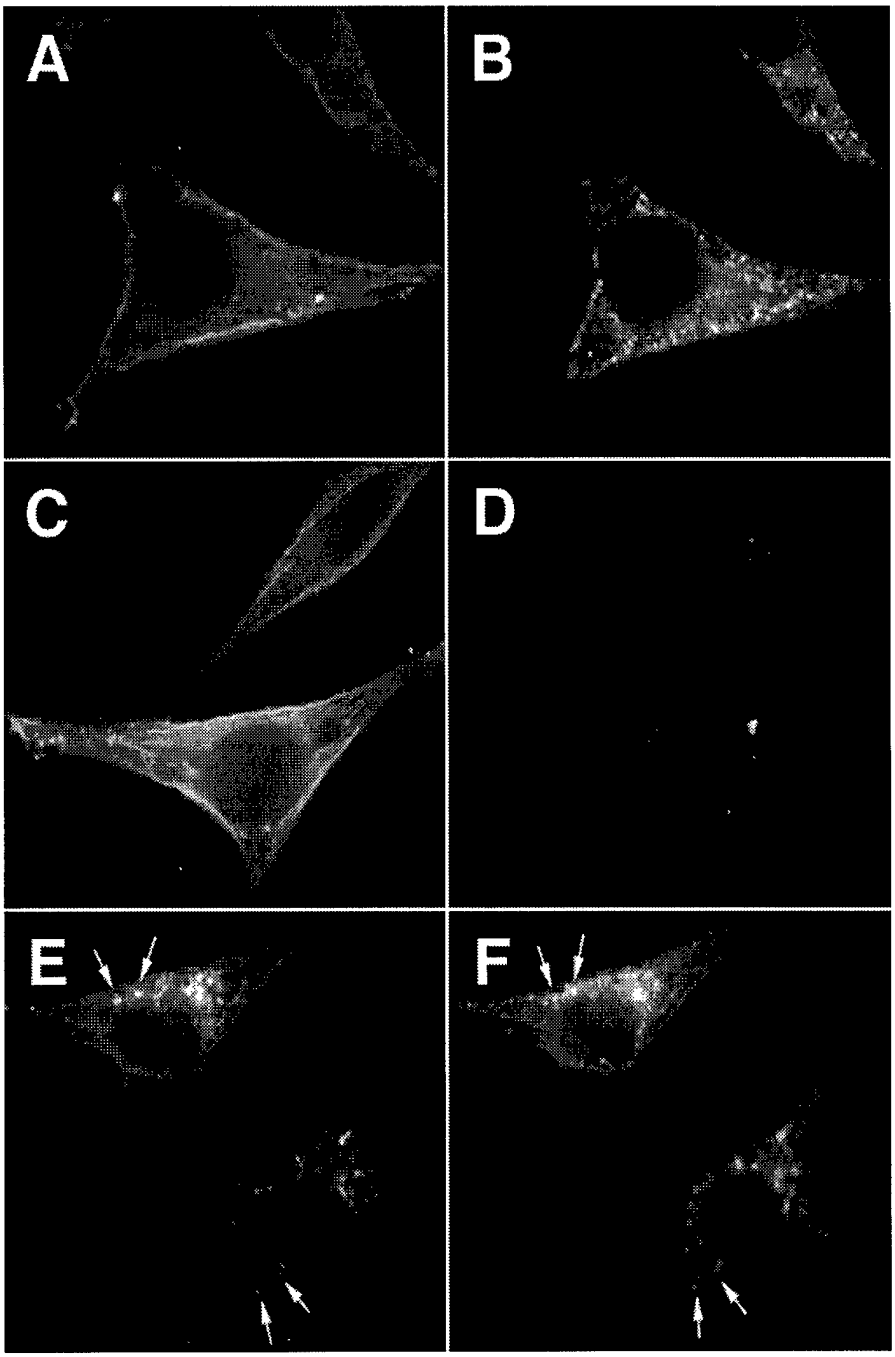

Figure 24

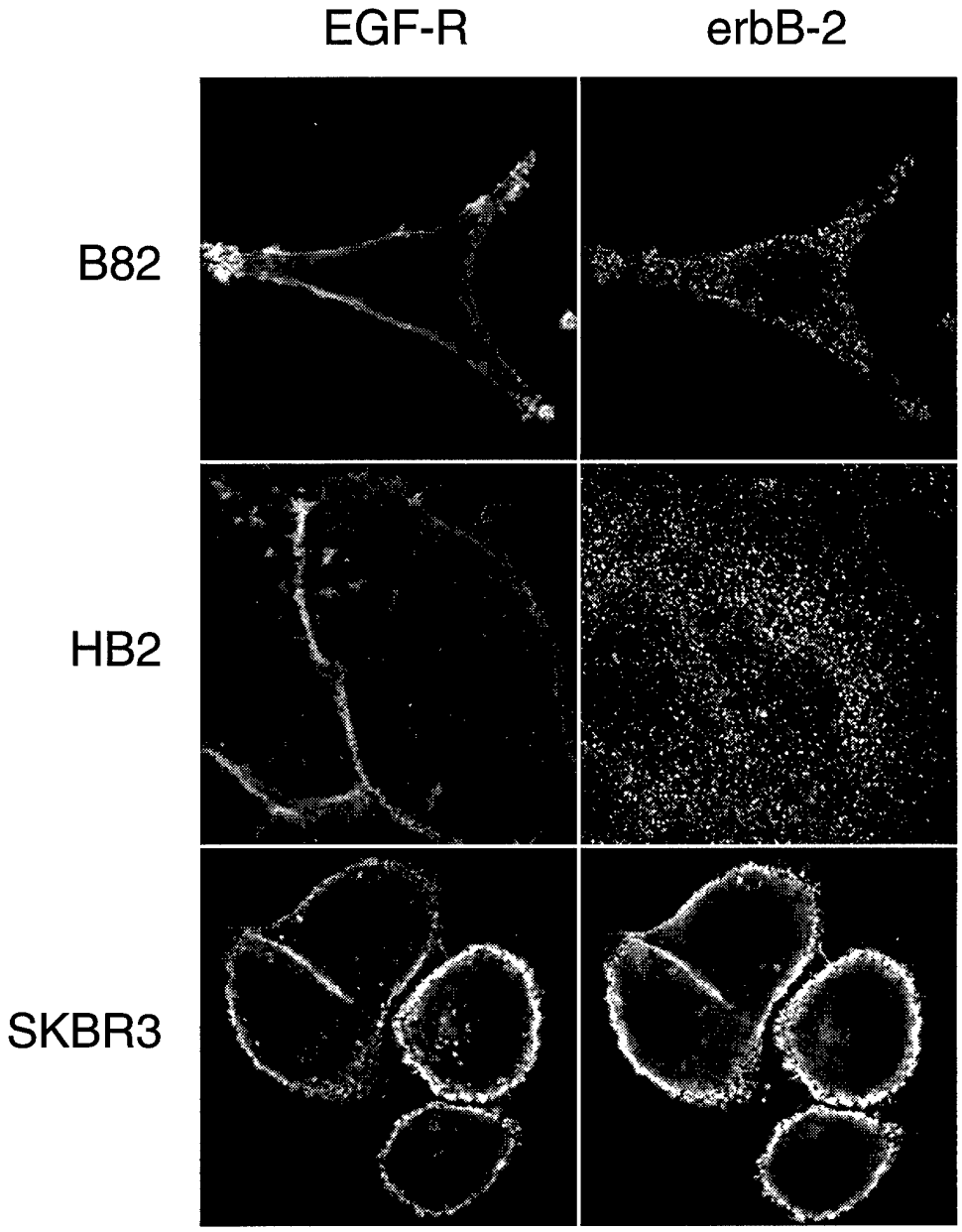

Figure 25

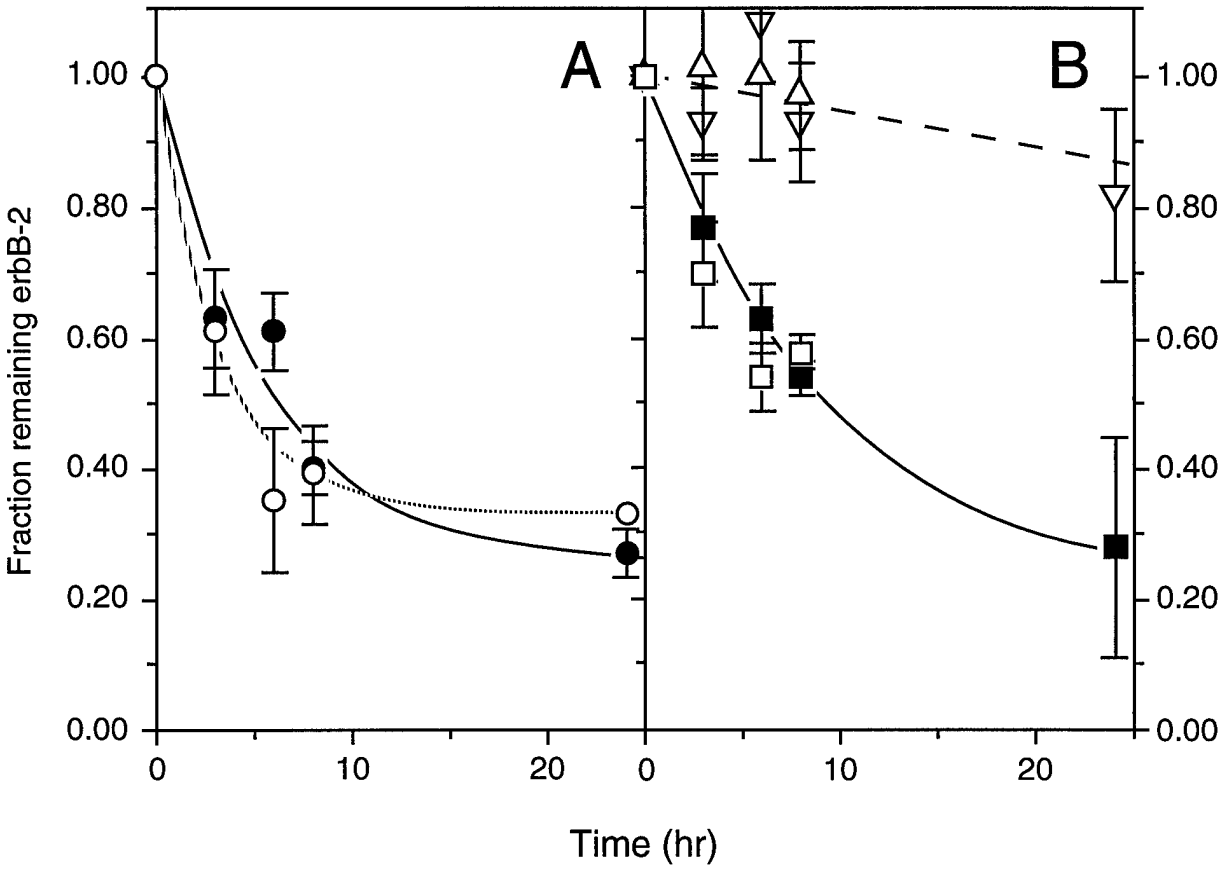
A
B
1.00
0.80
0.60
0.40
0.20
0.00
0
10
20
Fraction remaining erbB-2
Time (hr)

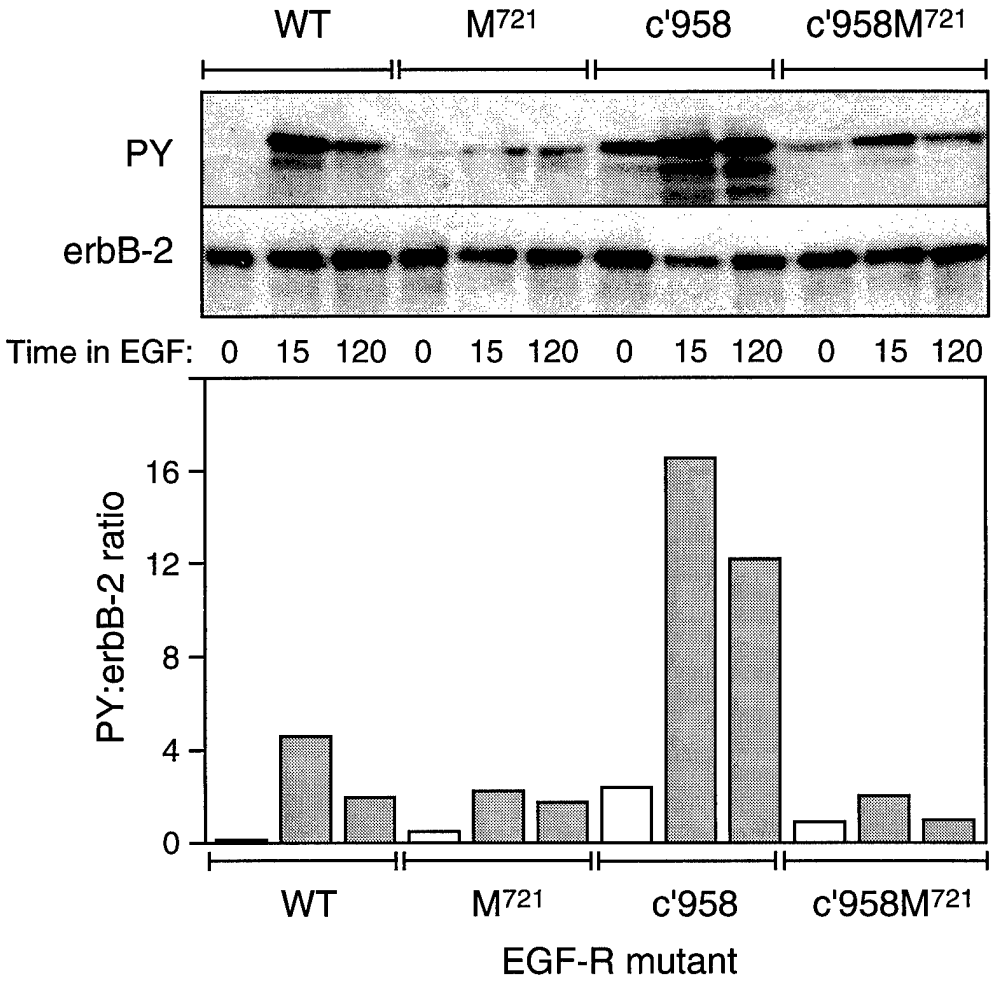
WT
M721
c'958
c'958M721
PY
erbB-2
Time in EGF: 0 15 120 0 15 120 0 15 120 0 15 120
PY:erbB-2 ratio
16
12
8
4
0
WT
M721
c'958
c'958M721
EGF-R mutant

Figure 27

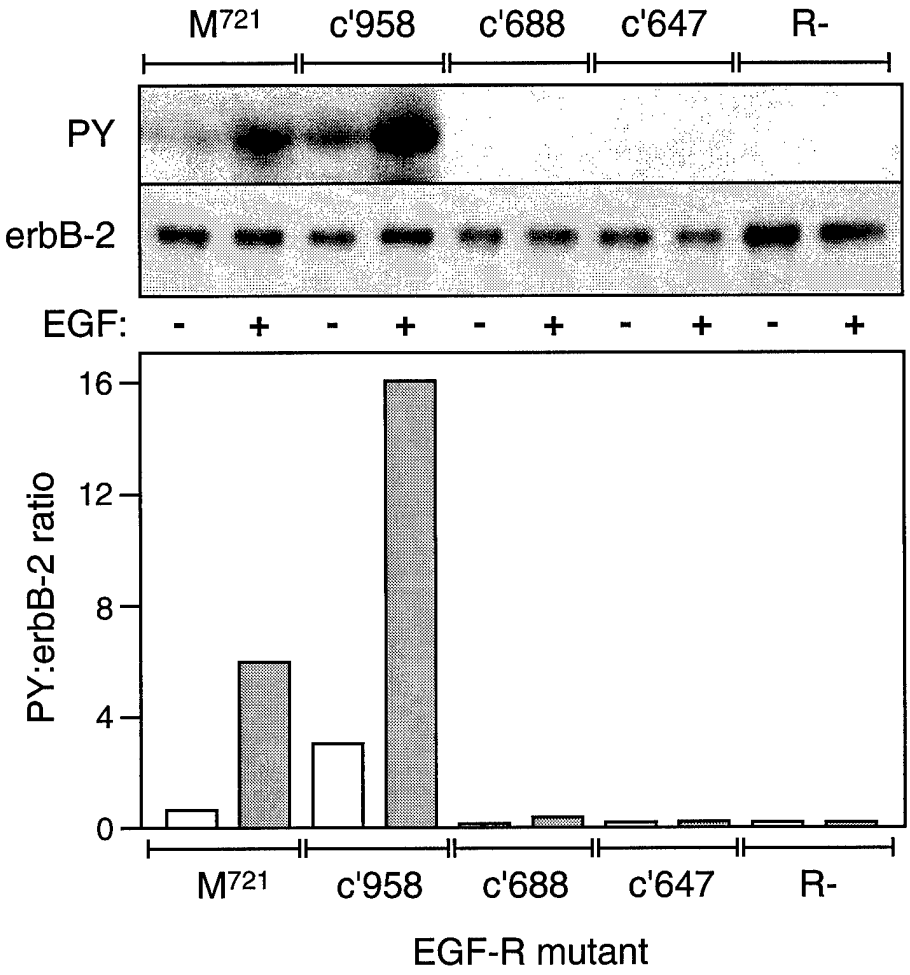
M721
c'958
c'688
c'647
R-
PY
erbB-2
EGF: - + - + - + - + - +
16
12
8
4
0
PY:erbB-2 ratio
M721
c'958
c'688
c'647
R-
EGF-R mutant

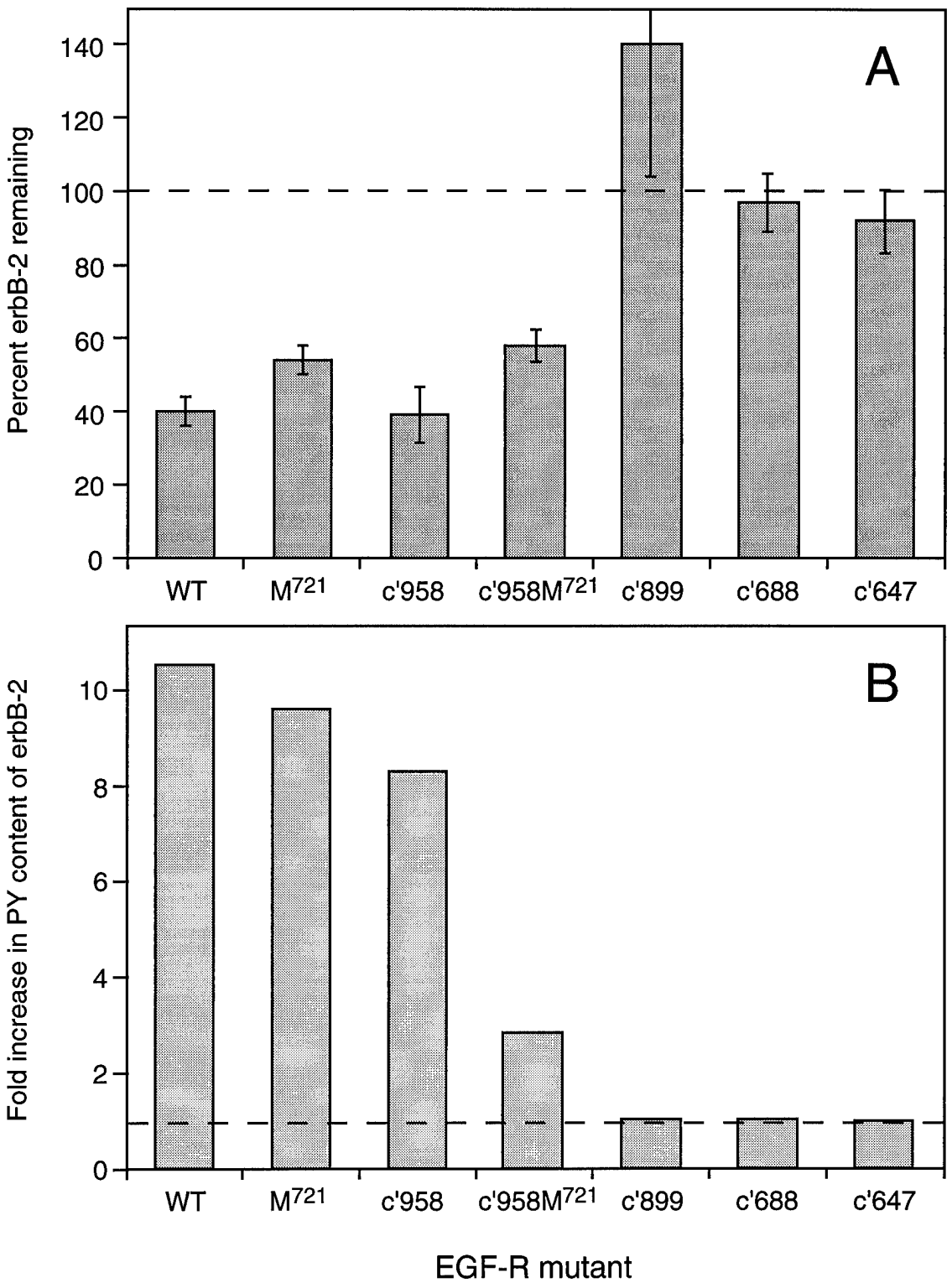
A
Percent erbB-2 remaining
140
120
100
80
60
40
20
0
WT
M721
c'958
c'958M721
c'899
c'688
c'647
B
Fold increase in PY content of erbB-2
10
8
6
4
2
0
WT
M721
c'958
c'958M721
c'899
c'688
c'647
EGF-R mutant